VIBRATION-BASED DAMAGE DETECTION AND SEISMIC PERFORMANCE ASSESSMENT

by

Ekin Özer

B.S., Civil Engineering, Bogazici University, 2009

Submitted to the Institute for Graduate Studies in
Science and Engineering in partial fulfillment of
the requirements for the degree of
Master of Science

Graduate Program in Civil Engineering

Boğaziçi University

2012

ACKNOWLEDGEMENTS

First and foremost, I would like to offer my sincere gratitude to my supervisor, Assist. Prof. Serdar Soyöz for the invaluable guidance, support and encouragement throughout my studies. Without his efforts and great contributions this thesis would not have accomplished. I would like to express my thanks to Assoc. Prof. Hilmi Luş for the advice and support since my first days in the university, and Assist. Prof. Ufuk Yazgan for his attention, time, and valuable suggestions.

I am also grateful to Assist. Prof. Kutay Orakçal for the continuous contributions during my undergraduate and graduate studies.

I am thankful to Prof. Maria Feng, and University of California, Irvine for sharing vibration data. Besides, I would like to thank Prof. Saidii's and Prof. Sander's NSF-NEES project, and University of Nevada, Reno where shaking table experiments are conducted.

Finally, I would like to show my greatest appreciation to my beloved parents, my sister, and İpek for their understanding, love and support when it was most required.

ABSTRACT

VIBRATION-BASED DAMAGE DETECTION AND SEISMIC PERFORMANCE ASSESSMENT

Reliability estimation is one of the key ingredients of performance evaluation and risk assessment strategies in structural and earthquake engineering. Residual life estimation is of great importance since design principles are constructed on a framework of performance-based engineering. Conventional methods of reliability estimation are mainly based on theoretical content without experimental information. System identification provides additional experimental information to update or verify analytical models by dynamic response measurements. Therefore, integration of system identification and reliability estimation could improve the accuracy of reliability estimation with rational and state-of-the-art information. In this study, a reliability estimation methodology, which incorporates vibration-based system identification, is presented. A two-span, three-bent reinforced concrete bridge structure is exposed to a series of white noise and earthquake excitations, and damage progress is documented. Two procedures are followed to modify base finite element model at different damage states. Updated procedure involves system identification and finite element model updating, whereas non-updated procedure is based on post-event structural parameter prediction using nonlinear time history analysis. For each damage state, updated and non-updated base models are used to estimate reliabilities by fragility curves. Fragility curves, considering peak ground acceleration as random variable, are estimated by a series of nonlinear time history analyses under various input ground motions. After all, the distinction between updated and non-updated fragility curves, and the effect of structural damage on fragility curves is disclosed. The results have proven that the proposed methodology, which utilizes system identification for reliability estimation, significantly changes estimation results and is essential for making accurate estimates of residual life.

ÖZET

TİTREŞİME DAYALI HASAR TESPİT VE SİSMİK PERFORMANS BELİRLEME

Güvenirlik tahmini, yapı ve deprem mühendisliğinde performans değerlendirme ve risk belirleme stratejilerinin en önemli öğelerinden biridir. Tasarım ilkeleri performansa dayalı mühendislik çerçevesinde oluştuğu için yapıların kalan yaşam süresini belirlemek oldukça önemlidir. Geleneksel güvenirlik tahmini metodları deneysel veriden yoksun teorik içerik üzerine temellenmişlerdir. Sistem tanılama, dinamik davranışı ölçümleyerek analitik modeli güncelleyecek ya da doğrulayacak deneysel bilgiyi sağlaya bilmektedir. Bu yüzden, sistem tanılama ve güvenirlik tahmininin birlikteliği güvenirlik tahmininin gerçekçi şekilde ve en ileri düzeyde bilgiyle yapılmasını sağlayabilir. Bu yüzden, bu çalışmada titreşime dayalı sistem tanılamayı içeren bir güvenirlik tahmini metodolojisi sunulmaktadır. İki açıklıklı, üç ayaklı bir betonarme köprü, bir takım beyaz gürültü ve deprem sarsıntılarına maruz bırakılarak hasarın ilerleyişi belgelenmiştir. Farklı hasar seviyelerinde güvenirlik tahmini yapmak için iki prosedür kullanılmıştır. Güncellenmiş prosedür sistem tanılama ve sonlu eleman modeli güncellemeyi içerirken, güncellenmemiş prosedür doğrusal olmayan zaman tanım analiziyle hasar sonrası yapısal parametrelerin tahminine dayanır. Güncellenmiş ve güncellenmemiş modeller, her bir hasar seviyesinde kırılganlık eğrileri aracılığıyla güvenirlik tahmininde kullanılmıştır. Etkin yer ivmesinin rasgele değişken kabul edildiği kırılganlık eğrileri, farklı yer sarsıntıları altında doğrusal olmayan zaman tanım analizleri yapılarak elde edilmiştir. Sonuç olarak güncellenmiş ve güncellenmemiş kırılganlık eğrilerindeki farklılık ve yapısal hasarın kırılganlık eğrilerine etkisi gösterilmiştir. Sonuçlar, sistem tanılamanın güvenirlik tahminlerinde kullanılmasını öneren bu yöntemin güvenirlik tahminlerini büyük ölçüde değiştirdiğini ve kalan ömrün doğru hesaplanmasındaki önemini ortaya koymaktadır.

TABLE OF CONTENTS

LIST OF FIGURES

LIST OF TABLES

LIST OF SYMBOLS

E	Modulus of elasticity
E_{cj}	28-day modulus of elasticity
EI	Stiffness
f	Frequency
f_{cj}	Compressive strength
F	Cumulative probability density function
g	Gravitational acceleration
h	Weighing coefficient for MAC value
Hz	Hertz
in	Inch
k	Weighing coefficient for modal frequency
K	Curvature
kN	Kilonewton
m	meter
mm	milimeter
M	Moment
MPa	Megapascal
P	Probability
rad	Radian
sec	Second
α	Bent stiffness modification factor
Δ	Drift
ψ	Mode shape
ξ	Damping ratio
ω_i	Angular frequency
π	Pi
θ	Rotation

LIST OF ACRONYMS/ABBREVIATIONS

EQ	Earthquake
FEM	Finite element model
MAC	Modal assurance criteria
NU	Non-updated
PGA	Peak ground acceleration
RC	Reinforced concrete
T	Test
U	Updated
WN	White noise

1. INTRODUCTION

1.1. Literature Review

Bridges are the most vulnerable parts of transportation networks, therefore, structural safety of bridges need to be carefully maintained. Collapse of such networks would lead to abruption of traffic flow, logistic turmoil, economical loss, and in the worst case, loss of human lives. Such vulnerability should be extensively considered especially in hazardous areas such as seismically active zones. Within the scope of structural and earthquake engineering, menaces provoked by structural failures should be clarified, in terms of performance evaluation, damage detection and seismic risk assessment of structures. In this context, reliability estimation goals to reveal residual life of structures in probabilistic manners. In case of decisions regarding the future of an existing structure, it is essential for the best usage of available sources.

Principles of performance-based engineering allows a limited extent of damage due to unexpected and disastrous events, mainly because of economical and architectural reasons. Therefore, it is necessitated to inspect the actual damage level of buildings, to state whether it is safe or not. Procedures for evaluation of existing structures have been developed, which are mainly based on analytical foundations. Even though concrete core testing is implemented into the procedure, it is suspicious to represent global characteristics of a structure with local experimentation. Apart from all these difficulties, structural health monitoring provides experimental information which reflects the system dynamic characteristics of a structure comprehensively. Such global characteristics of a system can be utilized by current performance evaluation and damage detection strategies. Furthermore, conventional post-event damage assessment methods such as visual inspection could be replaced or supported with system identification based methods. As a result, damage assessment could be conducted with a quick, quantitative, remote, computer-based and objective approach.

Therefore, two distinct disciplines, reliability estimation and system identifica-

tion could be unified to present a robust methodology with a rational perspective and advanced technology. Remarkable studies have been proposed related with these disciplines, and their intersection.

1.1.1. Structural Health Monitoring

Doebling *et al.*, (1996) provided a comprehensive review of structural health monitoring techniques and applications until 1996. The research motivation of structural health monitoring is to detect, localize, quantify and characterize structural damage indicated by changes in measured vibration response of structures. Within the improvement of these techniques, conventional methods such as visual inspection and localized experimental methods could be replaced or at least supported with global findings of health monitoring systems. A scheme is presented involving a sequential procedure such as "damage identification", "damage location", "damage extent", and "residual life estimation (not addressed)". Important statements are evaluated regarding the future of health monitoring of structures. It has been mentioned that automation, taking place of engineering judgment and analytical models, should be the ultimate goal; and more attention on nonlinear techniques should be paid. Once the dependence on prior test data or analytical models is avoided, much wider success, as in other applied fields such as rotating machinery, could be achieved. Furthermore, the ambiguity on number and location of sensors should be depleted, and sensitivity of measurements to modal characteristics should be revealed. Finally, efforts on real structures, and field tests under operating environment is encouraged. Nevertheless, several studies have shown that health monitoring is a prospective subject for the future of civil infrastructure, and may significantly contribute to the effective and safe use of structures.

Sohn *et al.*, (2004) presented a following review which also included the works completed from 1996 to 2001. The authors approached structural health monitoring as a statistical pattern recognition paradigm characterized by processes of "operational evaluation", "data acquisition, fusion, cleansing", "feature extraction and information condensation", "statistical model development". As mentioned in the previous review, major challenges awaiting structural health monitoring was determined. One of these

refer to the state where neither data nor analytical model is available, thus an unsupervised learning mode should be adopted. Another one was the ability to detect damage, which is a local phenomenon, through the global vibration response measurements of a structure. In addition to that, the ability to remove environmental and operational effects from actual structural damage was questioned. These challenges have to be dealt with in order to avoid negative and positive false indications, indications without the actual presence and no indications with the presence of damage, respectively.

Carden and Fanning (2004) presented another review which covered time and frequency domain methods. It has been stated that there are still great variety of approaches and disagreements regarding many different aspects of health monitoring. The diversity of algorithms, the sensitivity problems of modal parameter shifts, lackness of field tests, incapability of residual life estimations still stand as the fundamental problems, that health monitoring community needs to be dealt with. A special remark has been made on contribution of sensor numbering and locating. After all, as long as sensor number instrumented in a structure is limited, a unique or a single optimized solution is doubtful.

Brownjohn (2007) provided one of the most up-to-date reviews which discusses the goals of structural health monitoring, as well as previous works completed. Regarding the review, a classification is made based on types of structures. Furthermore, sensors used in structural health monitoring applications are considered in details. Finally, practical problems, recent capabilities and future motivations are determined.

1.1.2. System Identification

One of the earliest works in structural system identification, Shinozuka *et al.*, (1982), used artificially generated and experimentally obtained data to present estimations of unknown system parameters. The study involved parameter identification methods such as ordinary linear least-square, maximum likelihood, and instrumental variable methods to identify linear dynamic systems. It has been revealed that instrumental variable and maximum likelihood performed well even under noise, in contrast

with least square estimations. Furthermore, computational efficiencies of methods have been discussed. Yun and Shinozuka (1980), addressed nonlinear identification of dynamic systems. Parameter estimations are carried out with discrete and extended Kalman filtering algorithms, and iterated linear filter-smoothers. Artificially generated inputs, and outputs based on analytical simulations had been used to test the accuracy of the methods. It is concluded that performance of these methods is satisfactory even under high noise content, but with a moderate computational efficiency. Such works are extended with structural system identification methods and exemplary work by (Shinozuka and Ghanem, 1986), (Ghanem and Shinozuka 1995).

Kozin and Natke (1995) proposed a comprehensive review of system identification techniques both in time and frequency domains, and provided examples for better comprehension of proposed techniques. Maia and Silva (2001) reviewed and discussed identification techniques focusing on the use of experimental modal analysis results.

Safak (1991) introduced a system identification methodology which uses discrete-time filters, proper with the digitized form of measurement data. To document the verification of methodology, identification of a 12-storey building under 1971 San Fernando Earthquake is carried out. It has been shown that methodology is accurate, unless measurements contain narrow banded noise or nonlinearity. In such cases, an adaptive identification methodology should be used. Such methodology is addressed in Safak (1989); to develop an identification strategy which is robust even under noise with pre-dominant frequencies, time-varying characteristics, lack of information about system properties, and limited amount of data. Eventually, success of the identification procedure is validated with examples involving time- varying, nonlinear, and noisy conditions.

Celebi and Safak (1991), Safak and Celebi (1991) presented the dynamic characteristics of Transamerica Building, a 60-storey steel building with a pyramidal structure. Time history measurements are obtained during (1989) Loma Prieta Earthquake. Discrete-time linear filtering methodology is used for system identification. Findings including contribution of dominant modes and higher modes, and rocking phenomena

is represented.

Lus *et al.*, (1999) presented a system identification technique based on earthquake induced vibrational response measurement. The methodology adopted Eigensystem Realization Algorithm, and Observer/Kalman Filter Identification to identify dynamic characteristics of multi-degree of freedom structural systems. The validity of the methodology is discussed with case studies of an eight-storey building, and Vincent-Thomas cable suspension bridge responding to Whittier and Northridge Earthquakes. The immense performance of the proposed methodology have been presented in spite of noise in the measurements and inadequate number of sensors.

Beck and Katafygiotis (1998) targeted to achieve quantitatively documented accuracy in model predictions, with a methodology incorporating a Bayesian statistical framework into model updating procedure. The methodology is complemented with a secondary study inspecting model identifiability for multi-degree of freedom linear structural systems, addressed by Katafygiotis and Beck (1998). The core of the study, developing an algorithm to find alternative optimal models, is supported with numerical examples. The conclusions emphasize on the suspiciousness of model updating with single model, by questioning the uniqueness of such model, providing the existence of other optimal models.

Friswell *et al.*, (2001) discussed the parameterization and regularization process of finite element models to avoid misleading updating results. The necessity for physically interpreted parameters is emphasized as well as the ability to model the errors. Different approaches of model updating strategies was presented with a regularization effort on parameter boundaries. Methodologies are supplemented with examples to clarify the accuracy of the results.

One of the diligent studies targeting identification with the consideration of nonlinear and "unknown" systems was proposed by Masri *et al.*, (2000). Artificial neural networks had been used to identify changes in the structure by taking initial conditions as a reference. Without the presence of any prior information, the proposed method-

ology performed well in detecting damages. Introducing a prior model would enable quantification of damage.

Feng *et al.*, (2003) proposed a long-term monitoring methodology for bridge structures using neural networks. Such methodology was based on developing a baseline model which is based on training and testing of neural network, and extracting structural parameters from modal parameters. Such technique performed well in identifying structural parameters, in spite of insufficient number of sensors. Such baseline model could be used for future evaluation of performance of bridges.

Skolnik *et al.*, (2006) applied a system identification procedure using low-amplitude earthquake and ambient vibration data to obtain modal properties of a 15-story steel moment-resisting frame building. It is observed that identification results based on ambient vibration reflects a stiffer structure, in comparison with the results based on low-amplitude excitation. Finite element model updating, based on a modal sensitivity-based method, is carried out using system identification results under 2004 Parkfield Earthquake. Updated model's linear dynamic response under 1994 Northridge Earthquake is simulated to predict structural damage. Damage prediction is concluded to be insignificant, which agrees with report supplying 1994 damage assessment results.

Moaveni *et al.*, (2010) studied a 7-storey full-scale reinforced concrete building, which is exposed to progressively damaging seismic excitations imposed by a shake table. Ambient vibration and white noise excitation measurements, at different stages of damage, are processed to identify modal parameters. Sensitivity-based finite element model updating methodology is utilized to identify the presence, location, and extent of damage within the progression of tests. The findings state that identification, and updating results deviate from each other as ground motion intensities change. Increasing nonlinearity in response, with the increasing intensity, is the most probable source of such deviation.

1.1.3. Reliability Estimation

Park *et al.*, (1985) proposed a methodology to evaluate structural damage of reinforced concrete buildings under earthquake excitations. In this context, a relationship is established between earthquake intensity and structural damage. Furthermore, such procedure involved calibration based on damages of reinforced concrete buildings due to past earthquakes. Consequently, a quantitative damage assessment expression as a function of ground motion is presented. Such assessment involved probabilistic terms, which provided one of the keystones in reliability-based aseismic design.

Singhal and Kiremidjian (1998) introduced a Bayesian statistical analysis method to update the relationship between earthquake intensity and structural damage. Such analysis is conducted in the form of analytical fragility curve development. Furthermore, analytical fragility curves are combined with building damage data from past earthquakes. In this framework, analytical content stood for prior distribution, whereas data on building damage constituted likelihood function with the interference of Park and Ang damage index as a random variable. Eventually, updating is accomplished to obtain posterior distribution. Such updating strategy enabled to improve accuracy of fragility curves, which relies on periodic modification of reliabilities with the emergence of recently available damage data.

Shinozuka *et al.*, (2000) developed fragility curves of bridges with two approaches such as the one obtained from time history analysis, and the another one based on capacity spectrum method. Accordingly, fragility curves were compared. It was revealed that vulnerabilities identified from both methods lost the correlation as damage level rose from minor to major state. Such statement was presented as a result of increasing nonlinear effects with the increase of damage state. Nonetheless, adequate agreement was obtained between fragility curves of two different methods for high damage states. For low damage states, such agreement had proven to be excellent.

Shinozuka *et al.*, (2000) conducted a study which integrated analytical and empirical fragility curves in a statistical framework. In this study, analytical fragility curves

are constructed based on nonlinear dynamic analysis. Moreover, extensive data obtained from 1995 Kobe Earthquake is utilized for reconsideration of analytical fragility curves. As a conclusion, ability to obtain combined or composite curves is achieved, which leads to make widely representative fragility estimates, rather than case specific estimates.

Banerjee and Shinozuka (2008) attempted performance evaluation of bridges in a probabilistic manner. Quantitative measures of seismic damagability information is provided by an integrated procedure of empirical, analytical, and experimental approaches. Analytical study is performed with the incorporation of empirical information to produce a mechanistic model. Experimental data, with regards to physical damage descriptions, is obtained from a large-scale shaking table test. Finally, integration of analytical, empirical, and experimental results are proven to be consistent. Therefore, threshold limits for damage description in bridge columns is quantified and verified.

Frangopol *et al.*, (2008) presented an integrated procedure of structural health monitoring and reliability estimation. A practically applicable approach have been stated to make use of such integrated procedure. Furthermore, probabilistic prediction models could be developed in the light of health monitoring findings. Statements are provided with exemplary works, which are supported with an optimization framework for operational cost of health monitoring applications.

Catbas *et al.*, (2008) addressed a reliability estimation procedure with the inclusion of long-term structural health monitoring results. Monitoring of the longest span truss bridge in the US exposed that reliability excitations are significantly affected by changes in external loads and temperature. Findings of the study have shown the necessity of structural health monitoring for eliminating or reducing environmental uncertainties to obtain precise reliability estimation results.

1.2. Objective

A vast amount of research has been made in the subjects of structural reliability estimation and structural system identification, but few of them have spent efforts to combine these subjects together. Therefore, the relation between reliability and identified systems still have not discovered. Furthermore, it has been mentioned that the ultimate phase of structural health monitoring process is residual life estimation. Most of the comprehensive works have been omitted such phase, as few number of related studies exist in the literature. Therefore, there is a great need to enlighten the integrated use of reliability estimation and system identification, and discuss its contributions to the up-to-date structural and earthquake engineering mentality. For these reasons, the primary objective of this study is to investigate the influence of system identification on reliability estimation. In addition to that, investigation of damage progression's effect on residual reliability has been targeted. These objectives are pursued with an extensive methodology, involving testification of each components of the study, for maintaining the validity of the results.

1.3. Thesis Outline

This study is presented proper with the order of procedures followed throughout the experimental, analytical and post-processing phases. In the first chapter, a literature review regarding structural health monitoring, system identification and reliability estimation is presented. Furthermore, the scope and the objectives of work has been denoted.

In Chapter 2, experimental setup and testing procedures are explained. To summarize, a two-span, three-bent reinforced concrete structure is exposed to a series of earthquake and white noise excitations by three-shaking tables, synchronously. Measurements and observations documented the damage progression due to the excitations of increasing intensities.

Chapter 3 stands for the development and verification of finite element model of

the structure. Finite element model composing of plane elements and frame elements are compared, and chosen based on its accuracy and computational effort.

System identification methodologies are discussed in Chapter 4. Acceleration measurements, obtained from deck and columns of the bridge structure, is processed for structural system identification in frequency and time domain, and finite element model updating. The procedure constituted the development of "updated" finite element models for reliability estimation.

In Chapter 5, the details regarding nonlinear time history analysis are illustrated. As an alternative to system identification, nonlinear time history analysis is carried out for prediction of post-event structural parameters in terms of ductility demands. Similarly, "non-updated" finite element models are evaluated for reliability estimation.

In Chapter 6, a summary of the identification and nonlinear analysis results is made, and results are compared. Identified (updated) structural parameters are the bent stiffness values and damping ratio which are determined through a parametric study built on error minimization between simulated and measured models. Alternatively, nonlinear time history analyses are conducted to obtain predicted (non-updated) structural parameters in terms of effective stiffness and damping-damage relationship equations. Then these parameters, for each damage state, are presented in this chapter.

In Chapter 7, fragility curve development procedure and reliability estimation results are provided. Modified finite element models for each damage state are used for structural reliability estimation at the given state. For the purposes of reliability estimation, fragility curves, as a function of peak ground acceleration, are developed.

In the Chapter 8, conclusions are presented and the future work suggestions have been made. Eventually, the distinction between "updated" and "non-updated" fragility curves is examined to reveal the deviation of reliability estimation results due to different structural parameter values. The effect of structural damage on reliability estimation is also covered with the help of fragility curves obtained at different damage

states.

2. EXPERIMENTAL SETUP AND PROCEDURE

2.1. Dimensions and Material Properties

Experimental setup involves a quarter scale, two-span, three-bent reinforced concrete bridge structure Johnson*et al.*, (2006). Bridge deck consists of sizes such as 2.28 m in transverse direction, 18.28 m in longitudinal direction, and 0.36 m depth, as shown in Figure 2.1. Three equivalent beams are anchored to each other by post-tensioning to compose a rigid deck structure. Each bent consists of two circular cross-sectioned columns of a 0.305 m diameter, and all column cross-sections have the same dimensional properties. On the other hand, it is shown in Figure 2.2 that columns clear span differ from each other such as 1.83 m, 2.44 m and 1.52 for bent-1, bent-2, and bent-3, respectively. This results in different lateral stiffness values for each bent. Furthermore, Figure 2.3 shows that adjacent spans of the bridge structure is represented with additional masses located on the deck close to outer bents weighing 1190 kN in total. 28-day compressive strength of the superstructure is 35 MPa, whereas concrete cylinder tests results show a minimum of 31.9 MPa. Furthermore, reinforcement bars are defined by ASTM (American Society of Testing Materials) A706 specification such as Grade 60, referring to a yield strength of 420 Mpa.

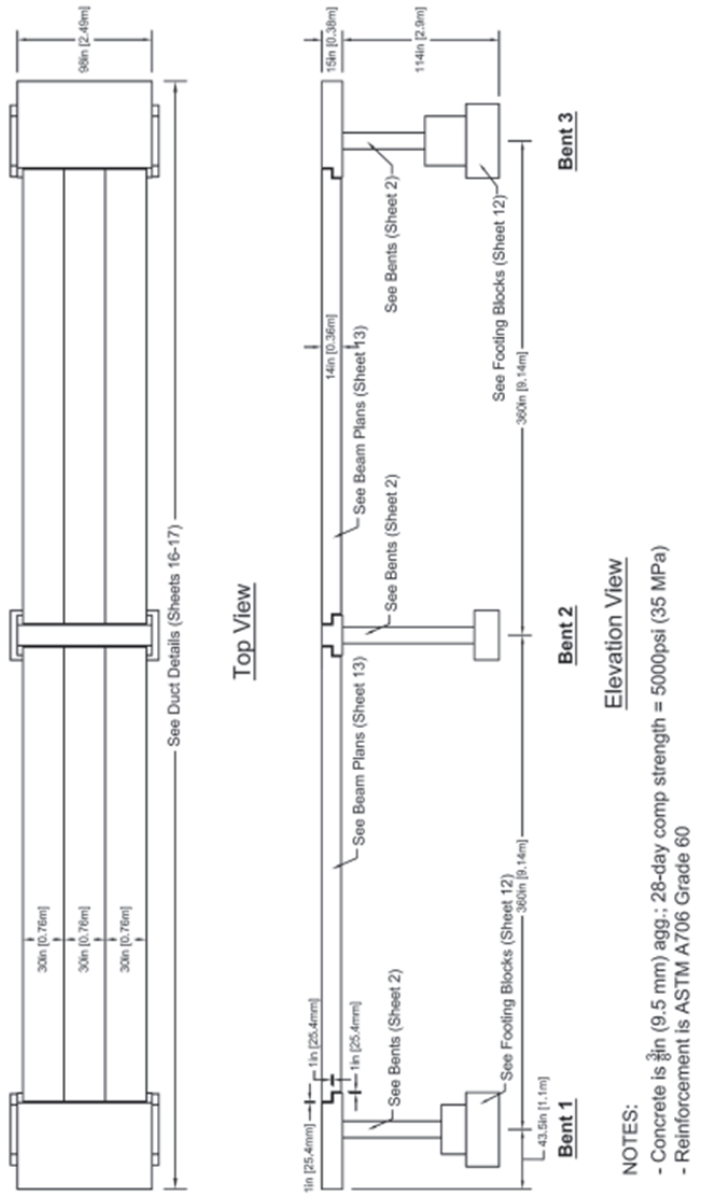

Figure 2.1. Top and elevation views of the bridge structure (Johnson *et al.*, 2006).

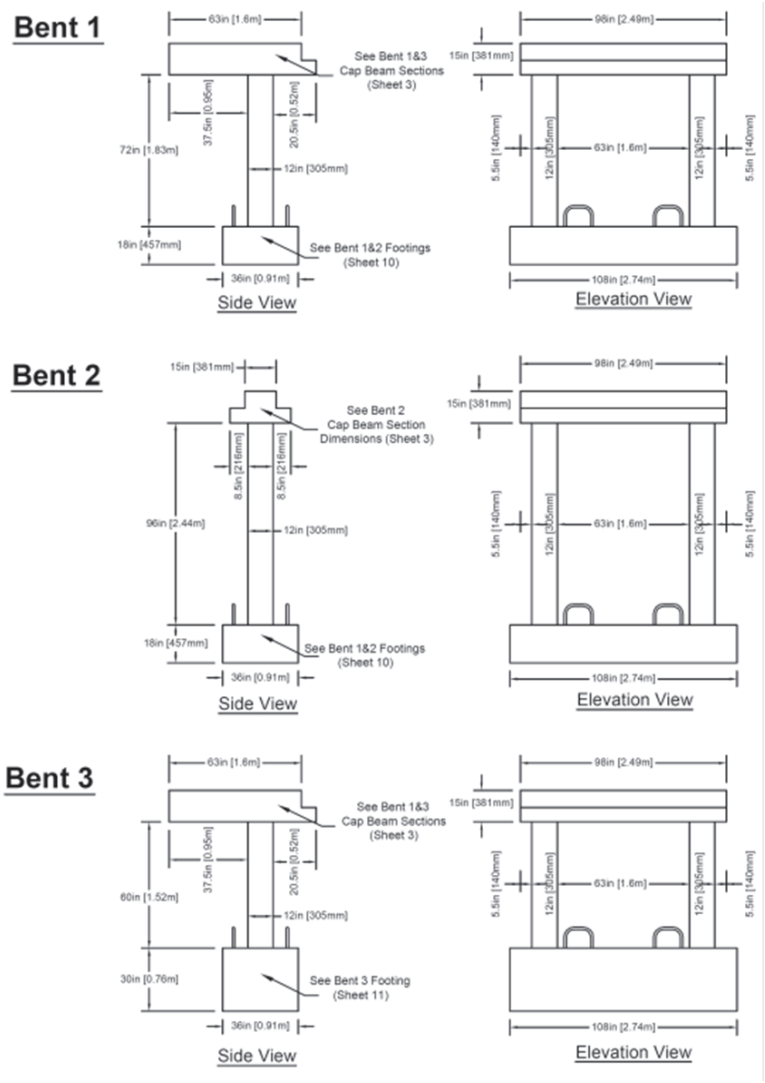

Figure 2.2. Side and elevation views of the bents (Johnson *et al.*, 2006).

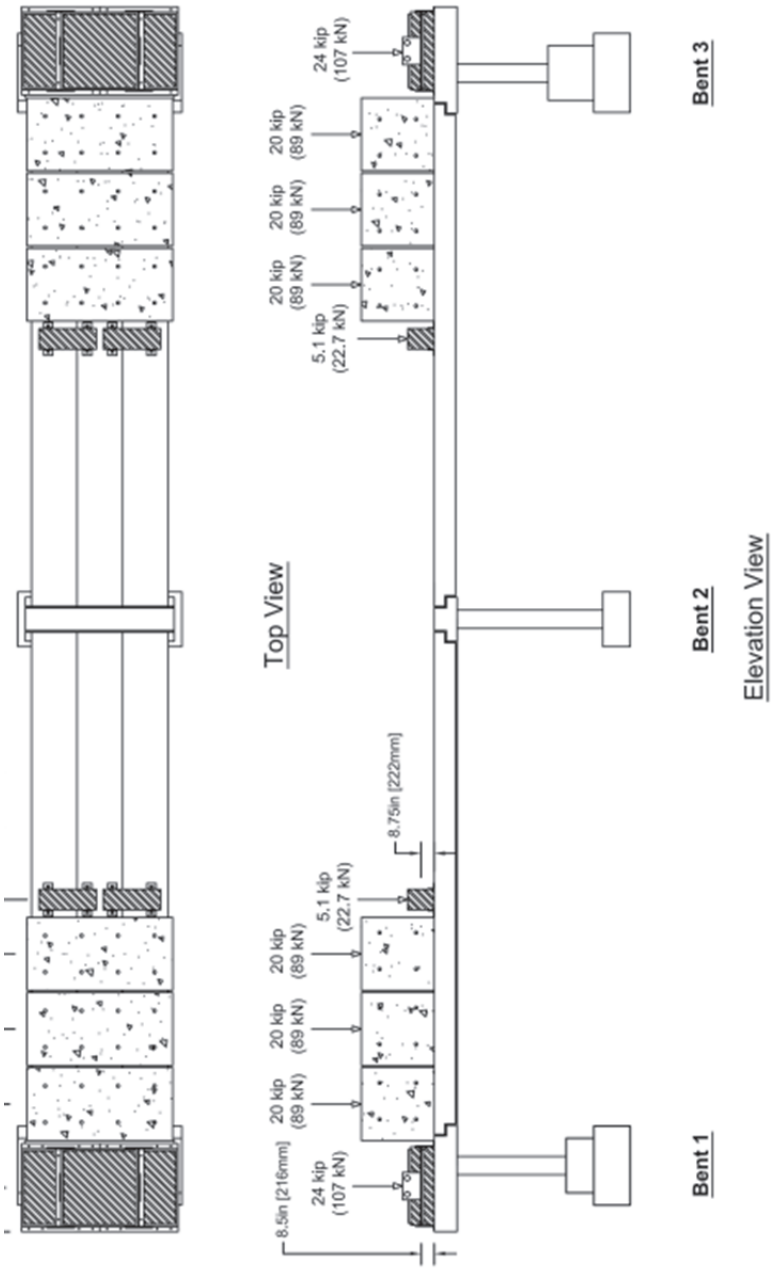

Figure 2.3. View of additional masses on the bridge structure (Johnson *et al.*, 2006).

2.2. Sensors and Shaking Tables

Vibration measurements in transverse direction are obtained with accelerometers located at eleven points on the structure, as shown in the Figure 2.4. This study uses data obtained from sensor 1, 4, 5, 6, 7, 8, 9 and 11 which provide adequate information for revealing transverse dynamic characteristics of the structure. Ground

motion inputs are measured by sensor 1, 6, and 9 which are located on the bottom of bent-1, bent-2 and bent-3, respectively. Output points are located on the deck, such as sensor 4, 7 and 11 providing acceleration data from the top of bent-1, bent-2 and bent-3, respectively; and sensor 5 and 7 providing acceleration on the midspans. 200 Hz of sampling frequency is used throughout the acceleration measurements.

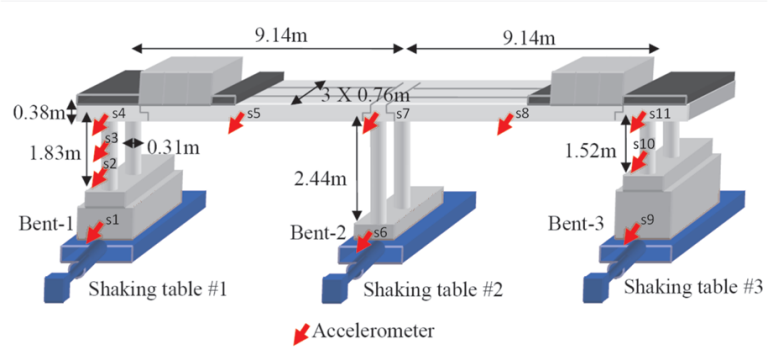

Figure 2.4. Bridge model and sensor layout.

2.3. Ground Motion Excitations

Shaking table test procedure is characterized by two types of excitations, earthquake and white noise excitations. Such discrimination is made based on the damageability and the frequency content of the excitations. Earthquake excitations are high amplitude dynamic events which result in structural damage, whereas white noise excitations does not cause any harm as they are low in amplitude. Excitations are imposed to the structure through bents, by multiple shaking tables. Each shaking table produces excitation on the corresponding bent, with the same target ground motion. Although target input accelerations are characterized by the same time history, a distinction between measured input accelerations is observed. Table 2.1 shows the deviation of achieved peak accelerations from target ground accelerations.

Progress of damage is documented based on the observations such as visual inspection and strain gauge measurements. The intensities of earthquake excitations increase proper with the application sequence such as T12, T13, T14, T15, T17, T18, and T19. Table 2.3 illustrates the excitation definitions, intensities, and damage obser-

Table 2.1. Target and achieved peak accelerations (Johnson, *et al.*, 2006).

	Table 1 (bent 1)			Table 2 (bent 2)			Table 3 (bent 3)		
Table motion	Target (g)	Achieved (g)	Achieved target	Target (g)	Achieved (g)	Achieved target	Target (g)	Achieved (g)	Achieved target
T1	0.15	0.21	1.34	0.15	0.32	2.09	0.15	0.25	1.63
T8	0.15	0.16	1.07	0.15	0.22	1.41	0.15	0.21	1.38
T12	0.08	0.07	0.94	0.08	0.10	1.29	0.08	0.08	1.09
T13	0.15	0.18	1.18	0.15	0.18	1.19	0.15	0.17	1.15
T14	0.25	0.35	1.39	0.25	0.31	1.25	0.25	0.28	1.12
T15	0.50	0.67	1.34	0.50	0.64	1.29	0.50	0.72	1.45
T16	0.75	0.98	1.31	0.75	0.94	1.25	0.75	1.25	1.67
T17	1.00	1.20	1.20	1.00	1.50	1.50	1.00	1.09	1.09
T18	1.33	1.56	1.17	1.33	1.81	1.36	1.33	1.59	1.19
T19	1.66	2.00	1.20	1.66	2.13	1.28	1.66	2.20	1.33
T20	1.00	1.26	1.26	1.00	1.30	1.30	1.00	1.43	1.43

vations from the sequentially conducted tests. Figure 2.5 show the entire input ground motion time history including both white noise and earthquake excitations. Figure 2.6, Figure 2.7, and Figure 2.8 illustrates input motions both in time and frequency domain. From these figures, it could be commented that white noise excitations contains low amplitude ground accelerations and broad band frequencies, whereas earthquake excitations are high amplitude input motions with pre-dominant, narrow band frequencies. Such phenomena is expected due to the concept of such types of excitations.

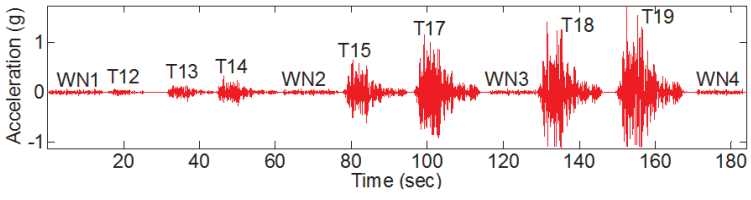

Figure 2.5. Input motions.

Table 2.2. Test procedure.

Test ID	Ground Motion	PGA (g)	Damage Description
WN-1	White Noise	0.07	
T-12	Low EQ	0.07	
T-13	Low EQ	0.18	Bent-1 yields
T-14	Moderate EQ	0.33	Bent-3 yields
WN-2	White Noise	0.07	
T-15	High EQ	0.64	Bent-2 yields
T-17	Severe EQ	1.15	
WN-3	White Noise	0.07	
T-18	Severe EQ	1.40	
T-19	Severe EQ	1.74	Bent-3 buckles
WN-4	White Noise	0.07	

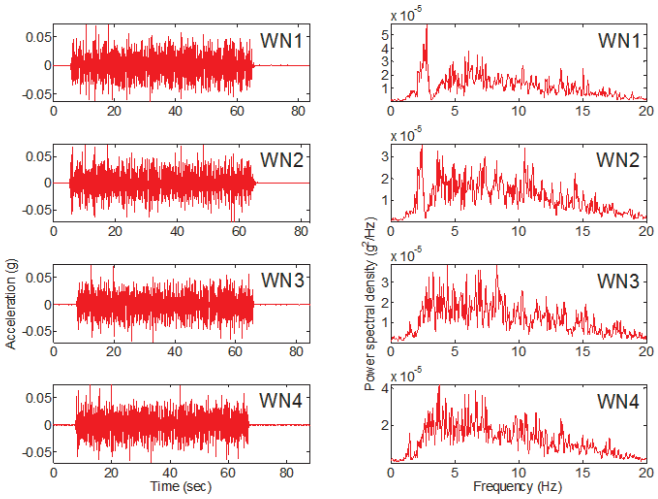

Figure 2.6. Time histories and Fourier spectra of white noise excitations.

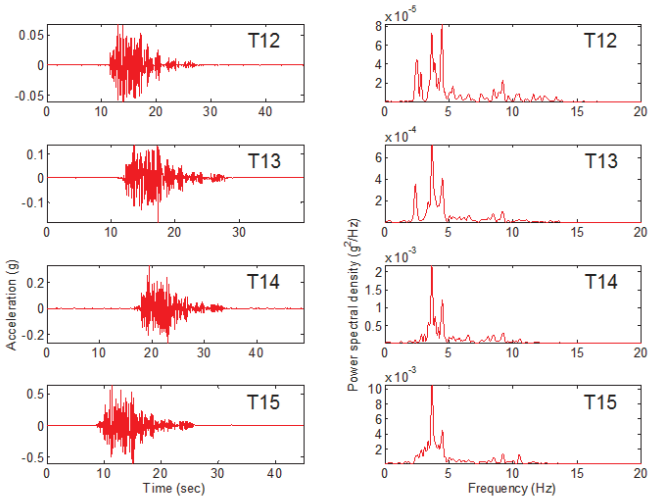

Figure 2.7. Time histories and Fourier spectra of low, moderate and high earthquake excitations.

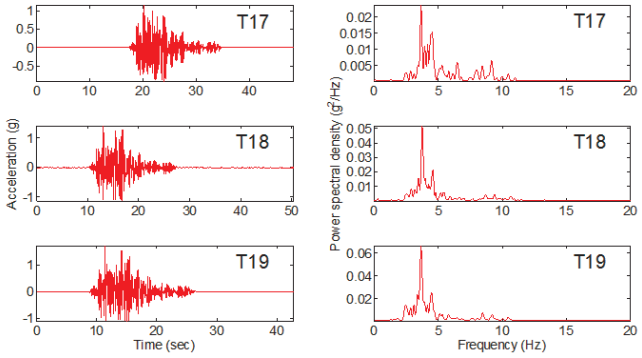

Figure 2.8. Time histories and Fourier spectra of severe earthquake excitations.

2.4. Observed and Measured Damage Progress

Due to the additional masses and low flexibility at outer bents, dynamic characteristics of structure is defined by irregular torsion demanding transverse movement. For this reason, outer bents, bent-1 and bent-3 experience critical damage, compared with bent-2 located in the middle. Damage propagation is frequently documented with crack mark photos, such as shown in the Figure 2.9 and Figure 2.10. Detailed documentation and comprehensive information about the experiment can be found in (Johnson *et al.*, 2006).

Figure 2.9. Damage observed on bent-1 after T13, T14, T15, T19; respectively (Johnson *et al.*, 2006).

Figure 2.10. Damage observed on the lower and upper portion of bent-3 after T19 (Johnson *et al.*, 2006).

Visual inspection results documented by crack mark photos and curvature measurements are used to investigate the damage progression on the upper and lower ends of the columns. Figure 2.11, and Figure 2.12 illustrates the crack propagations at the upper and lower ends of bent-1 throughout all tests. Illustrations show that the comparison of damage severity between lower and upper ends is not very distinctive.

Information of curvature is of great importance due to the fact that it is one of the chief indicators of structural damage on columns. Therefore, comparison of damage progression on column ends could be made based on curvature measurements at column ends. In accordance to that, curvature measurements shown in the Figure 2.13 and Figure 2.14 provide curvature time histories at upper and lower ends of bent-1. These figures point out that curvature time histories, therefore, damage progression on the lower and upper column ends are compatible. This provides the possibility to define the damage index of a column or bent with a single parameter, representing both of its top and bottom ends. The incorporation of such finding into system identification,

finite element model updating and nonlinear time history analysis will be discussed in the further chapters.

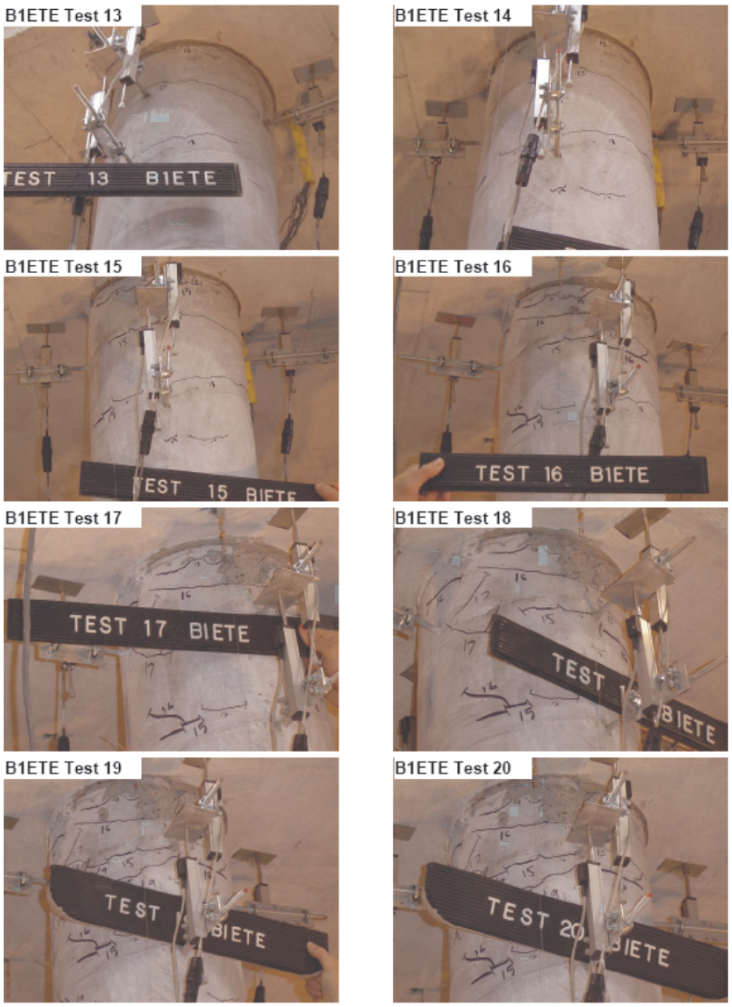

Figure 2.11. Crack propagations on the upper portion of bent-1 columns (Johnson *et al.*, 2006).

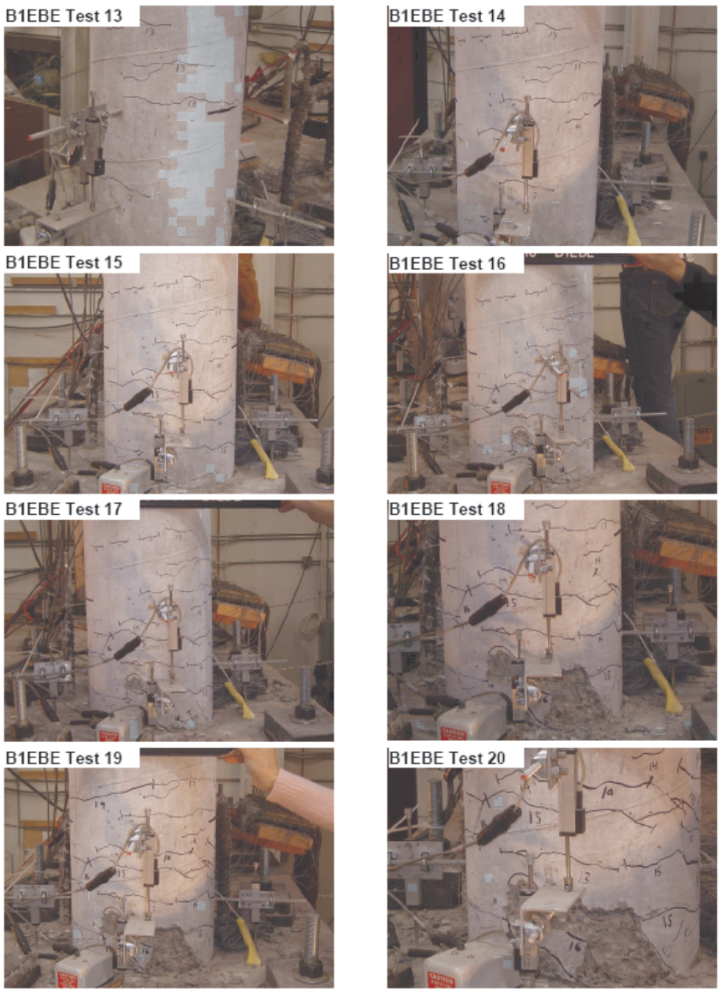

Figure 2.12. Crack propagations on the lower portion of bent-1 columns (Johnson *et al.*, 2006).

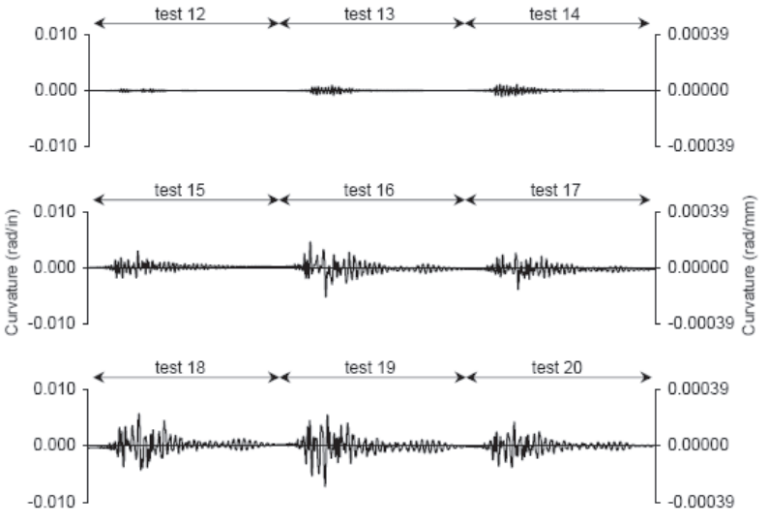

Figure 2.13. Curvature history for upper portions of bent-1 columns (Johnson *et al.*, 2006).

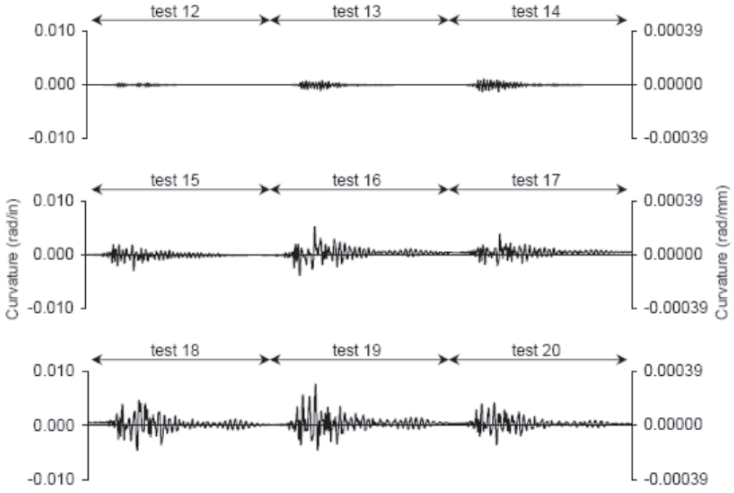

Figure 2.14. Curvature history for lower portions of bent-1 columns (Johnson *et al.*, 2006).

3. FINITE ELEMENT MODEL OF THE STRUCTURE

3.1. Inspection of Alternative Finite Element Modelling Approaches

This section explains the finite element modelling procedure of the structure. The discussion involved in this section is essential to demonstrate the validity of modelling approaches. Finite element modelling and analyses are carried out with the structural analysis program, SAP 2000 version 10. Extrude view of Model 1 discussed below is shown in the Figure 3.1. Design drawings provide adequate information regarding the element dimensions and masses. Bents are represented with two columns connected with each other by a beam element. Furthermore, deck elements connect each bent element to form the bridge structure.

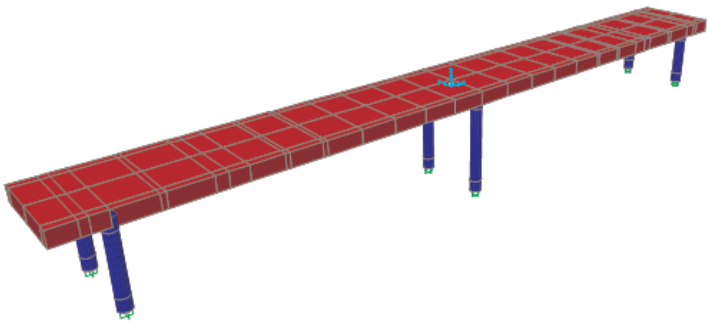

Figure 3.1. Extrude view of finite element model.

Modulus of elasticity of reinforced concrete is expressed by many different design codes and regulations in terms of 28 day strength of concrete. The American Concrete Institute(ACI) Code (2008), Eurocode 2 (2005) and Turkish Standards (TS-500) provides Equation 3.1, Equation 3.2 and Equation 3.3, respectively, such as

$$E_{cj} = 4700.\sqrt{f_{cj}}, \tag{3.1}$$

$$E_{cj} = 9500.(f_{cj} + 8)^{1/3}, \tag{3.2}$$

$$E_{cj} = 3250.\sqrt{f_{cj}} + 14000, \tag{3.3}$$

where E_{cj} is the modulus of elasticity, f_{cj} is the compressive strength.

Reinforced concrete class used in this experiment is 35 Mpa which refers to a modulus elasticity of 27800, 33300, and 33200 Mpa according to the ACI Code, Eurocode 2, and TS500, respectively.

Additional masses anchored to the structure are assigned as joint masses, shown in Figure 3.2. Masses, due to deck's unit weight, are modelled with joint masses by distribution of total deck mass into 25 joints. Such discretization is done considering the trade-off between computational speed and accuracy. In Table 3.1, comparison of discretized (Model 2) and uniformly distributed (Model 3) mass models show that such simplified model is capable of representing the original model

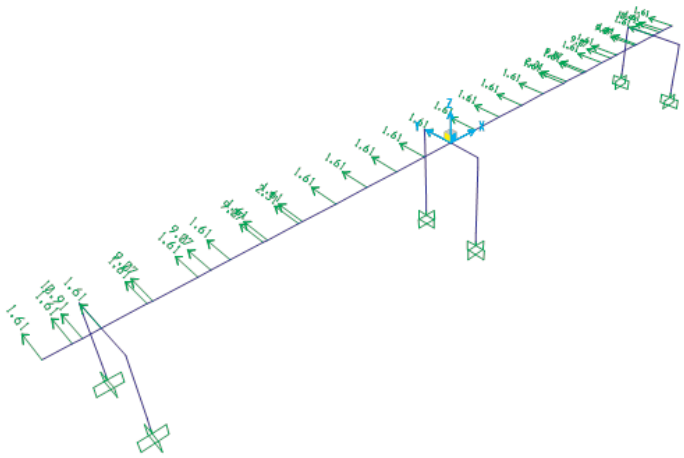

Figure 3.2. Mass distribution in finite element model.

Columns and beam elements are defined as frame elements with section and length dimensions according to design drawings. Two different approaches are considered in development of deck element to represent actual structure with accuracy and efficiency.

These approaches are distinct from each other for idealization of the deck element, such as either plate or frame finite elements. Model 1 is developed by meshing of deck structure into rectangular plate elements. It should be noted that size and shape of meshes are effective in convergence of a model. Fine and square-like rectangular meshes leads to accuracy, but high mesh numbers would increase computational time of analyses. Accordingly, meshing properties of Model 1 could be investigated according to Figure 3.3. In Model 2, deck is developed with frame elements, which is simple but questionable. The reason for doubt is that deck's one of the cross-sectional dimensions is quite large compared with element length, which is theoretically contradictory for frame elements. Therefore, its performance should be revealed by a comparison with Model 1. Figure 3.3, shows the graphical interpretation of Model 1 and Model 2. Finally, a conversion of Model 2 into uniformly distributed mass is developed with the name of Model 3 to understand the effect of discretization in mass.

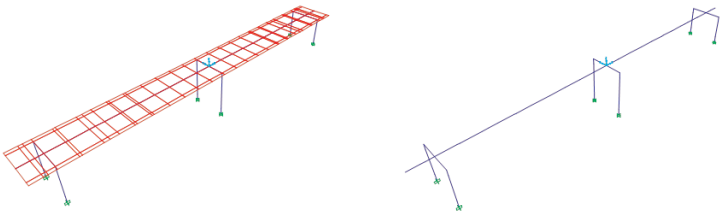

Figure 3.3. Idealizations of Model 1 and Model 2, respectively.

Based on modal frequency comparisons of Model 1, Model 2; Table 3.1shows that representation of bridge deck is possible with frame elements, as well as plate elements. Furthermore, discretization number of masses in Model 2 is concluded to be adequate as modal frequencies due to Model 2 very close to Model 3. In addition, as shown in the Figure 3.4 mode shapes obtained from Model 2 are perfectly compatible with other models. Therefore, a modelling strategy such as in Model 2 is valid and could be adopted to develop the actual model in OpenSees.

Table 3.1. Modal frequencies of finite element models.

	f_1 (HZ)	f_2 (HZ)	f_3 (HZ)	f_4 (HZ)	f_5 (HZ)
Model 1	4.1346	5.4137	13.5433	28.6993	56.2634
Model 2	4.1333	5.4113	13.5446	28.7439	56.6251
Model 3	4.1012	5.4573	13.6309	29.2312	55.7103

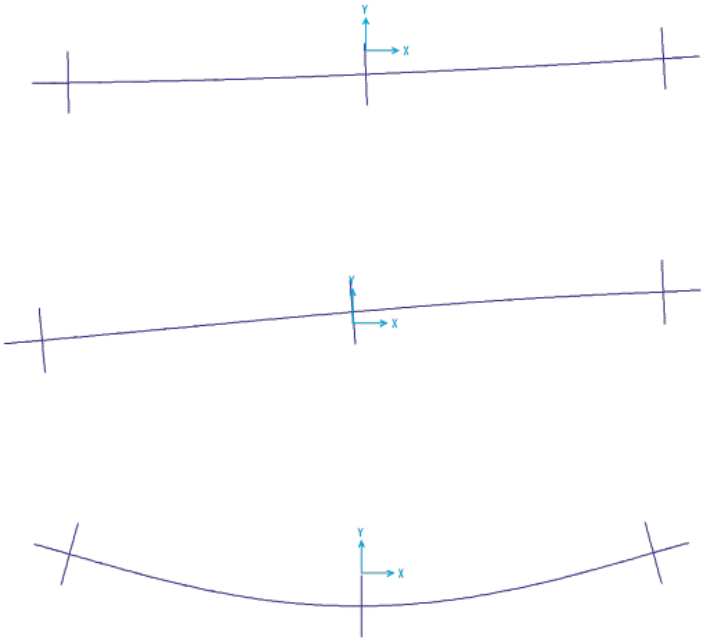

Figure 3.4. Mode shape 1, 2, 3, respectively (SAP2000).

3.2. Influence of Modes of Vibration on the Structural Response

The influence of modes on vibrational characteristics of the structure is investigated by inspection of modal participations. Such observation is essential for consideration of error functions in frequency domain identification which will be discussed in the following section. Table 3.2 presents modal participation ratios extracted from Model 2. According to the table, it is apparent that mode-1 is the pre-dominant mode, which needs to be represented in high accuracy as its dynamic participation ratio is 83%. Therefore, identification of mode-1 is should to be done with cautiousness. In addition, incorporation of mode-1 and mode-2 constitutes 99% of the structural response. With the introduction of mode-3, response is represented with 100% par-

ticipation. Therefore, no further modes need to be investigated, or implemented into identification procedure.

Table 3.2. Modal participation ratios.

Contributary modes	Modal participation ratio (%)
1	82.864
1, 2	99.399
1, 2, 3	99.996
1, 2, 3, 4	99.998
1, 2, 3, 4, 5	100.000

3.3. Verification of OpenSees Model with SAP2000 Model

OpenSees platform is an open-source software of earthquake engineering simulation developed by McKenna *et al.*, (2004). Elastic Beam Column elements are used for modelling columns and beams. Eigenvalue analysis is carried out to obtain modal parameters Mazzoni *et al.*, (2007). First five modal frequencies are obtained such as 4.27, 5.64, 13.83, 30.71 and 64.76. It is concluded that modal values obtained from OpenSees and SAP2000 agree to a good extent, but a slight difference is observed. Mode shapes obtained from OpenSees correlates with SAP2000 results, as it seen from the Figure 3.4 and Figure 3.5.

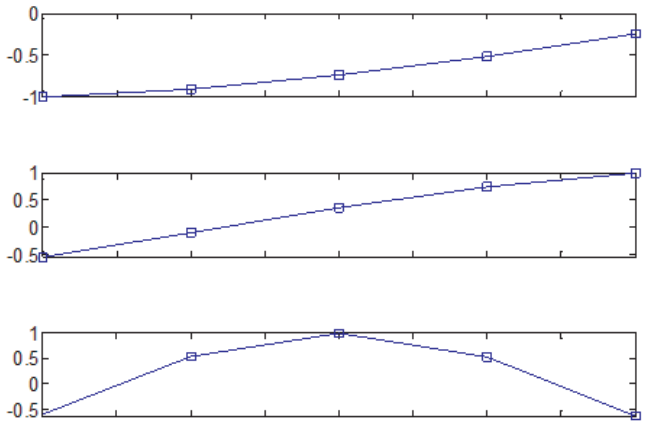

Figure 3.5. Mode shape 1, 2, 3, respectively (OpenSees).

A final comparison to verify OpenSees model is shown in Figure 3.6. In this figure, acceleration time history of sensor 4 location, as a response to WN1 excitation, is illustrated. Linear time history analyses are carried out via SAP2000 and OpenSees. The figure shows that finite element model developed in OpenSees is in correlation with model developed in SAP2000. Thus, verification of OpenSees model is achieved.

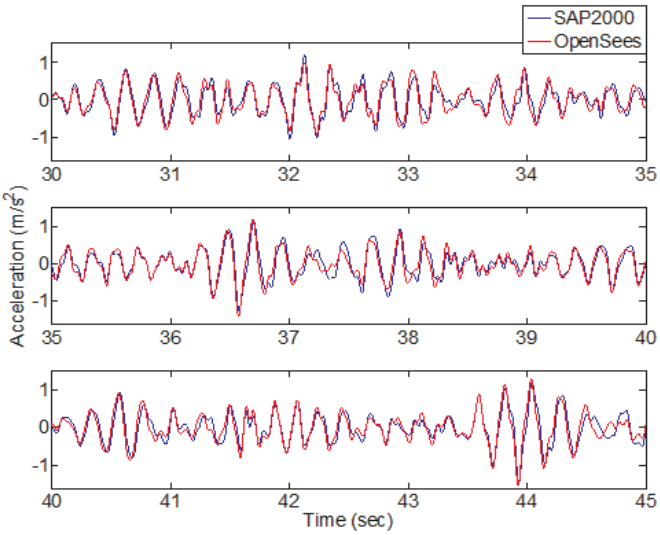

Figure 3.6. Acceleration time history response obtained from SAP2000 and OpenSees.

3.4. Parametric Study with the Integrated Use of Matlab and OpenSees

This section targets to reveal the finite element model updating procedure which is based on an integrated computational process operating Matlab and OpenSees. OpenSees is a finite element model software developed with object-oriented approaches. OpenSees is supported by a script-based computer language "Tcl" which provides a wide range of usefulness in terms of variable handling, and mathematical procedures. The most efficient use of OpenSees requires generating models through text-scripts and "sourcing" such scripts in need of use, instead of direct commanding of inputs at the prompt screen (Mazzoni *et al.*, 2007).

Matlab is a computing language and numerical analysis program which is capable of executing external computer programs. Furthermore, it is capable of either creating new, or changing existing text files. Therefore, it is provides a useful environment for

handling finite element analysis procedure executed by OpenSees. With the interference of Matlab, inputs and outputs of analysis could be controlled, and obtained data could be extracted, stored and post-processed. With the presence of a loop algorithm, such interference could be repetitively commanded by no human intervention. Such an algorithm is developed to run enormous number of analysis in a remote fashion. As a result, the basis for a parametric study, to be used in system identification procedure, is constructed. In the Figure 3.7, the interaction between Matlab and OpenSees programs is illustrated which compose a thorough parametric study. Initially, parameters are generated by Matlab and introduced to the OpenSees. Using these parameters, OpenSees executes the finite element analysis, and returns the structural responses of interest. Finally, Matlab takes and evaluates the structural response to compute the error which corresponds to the specific parameter combination. Finally, error is stored, the parameters for the next run are generated, and sent to OpenSees for the new finite element analysis. Such procedure is succeeded repetitively by developing and coding a loop algorithm for parameter generation. The analysis provided in the following sections are based on such an integrated computational procedure.

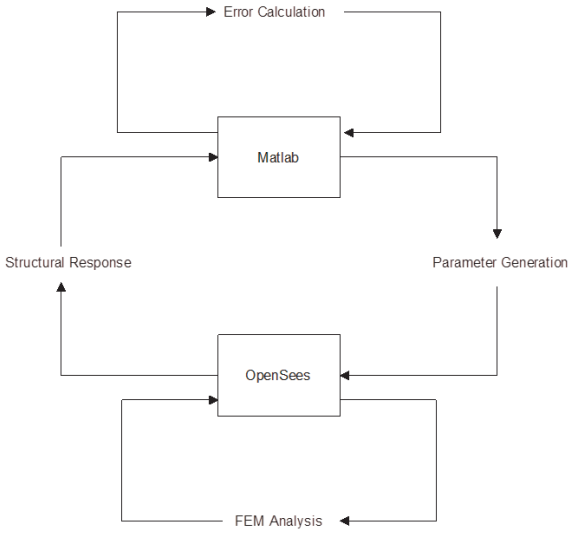

Figure 3.7. Scheme describing integrated use of Matlab and OpenSees.

4. SYSTEM IDENTIFICATION

4.1. General

System identification methods could be basically divided into two groups such as frequency domain methods and time domain methods. In this study, system identification is carried out in both domains. Vibration measurements obtained from the structure during white noise excitations, which are low amplitude and non-damaging events, are used for system identification purposes. For this reason, structural system is linear time-invariant, and there is no initiation of structural damage during white noise excitations.

Based on design drawings and code requirements, prior finite element model is developed in OpenSees platform. Inspecting the main structural components, deck and bents, it could be commented that the majority of the damage would take place on columns, rather than deck. Moreover, distribution of damage would not be uniform for columns. Instead, damage would be concentrated on column end regions, where plastic deformations are apparent. Followingly, structural parameters should be determined to represent the structural damage to the best extent. Therefore, it is reasonable to parameterize each bent stiffness so that structural damage on columns could be described by changes in such parameters. Accordingly, bent stiffness values are to be multiplied by three modification factors, α_1, α_2, α_3, to refer to the identified structural stiffness of bent-1, bent-2, and bent-3, respectively.

Two main considerations for parameter identification are identification in initial state, and identification in damaged state. Identification in initial state refers to the state where no structural damage is expected. Therefore, identified parameter should encompass the whole length of the column, as material and inertial properties are supposed to be the same for any section along the total length of a column. Apart from that, identification of parameters in damaged states should be able to reflect the change in the damaged portion of a column, therefore it should be carried out for

column end regions. In such states, as damage initiation is not expected on the middle portions of columns, initially identified modification factors are kept constant.

Based on the prior finite element model, and parametrization procedure described above, a set of candidate models are generated. Each structural parameter ranges between the selected minimum and maximum coefficients. The upper limit is set to 1 as post-event stiffness can not exceed pre-event stiffness. The lower limit may vary according to the frequency content, duration, and intensity of earthquake excitation and vibrational characteristics of structure. In this study, a lower limit of stiffness modification, 0.2 is found to be adequate for reasonable system identification results. Therefore, parameter range between 0.2 and 1.0 is concluded as reasonable to cover varying damage possibilities. Damping ratio, ξ, emerges as another structural parameter which is only considered in time domain identification. Similarly, a parameter range which centers the previously identified damping ratio is generated for time domain identification processes. For the initial state, as 5% damping ratio is expected for reinforced concrete buildings, identification is initiated with such value. The relationship of damping as a structural parameter and Rayleigh Damping is presented with the Equation 4.1, Equation 4.2 and Equation 4.3;

$$C = \alpha.M + \beta.K, \tag{4.1}$$

where C is the damping matrix, M is the mass matrix, K is the stiffness matrix.

The coefficients, α and β, involve damping ratio parameter such as

$$\alpha = \xi.\frac{2.\omega_i.\omega_j}{\omega_i + \omega_j}, \tag{4.2}$$

$$\beta = \xi.\frac{2}{\omega_i + \omega_j}, \tag{4.3}$$

where ω_i is the ith modal frequency, ω_j is the jth modal frequency, ξ is the damping

ratio.

4.2. Digital Signal Processing

4.2.1. Signals in Time Domain

A signal could be comprehended as a function composed of series of periodic functions. Such periodicity could be expressed in terms of sinusoidal and cosinusoidal functions with different amplitudes and frequencies. Therefore, such signals could be represented with Fourier series, consisting of infinite series as in the Equation 4.4

$$x(t) = \frac{a_o}{2} + \sum_{n=1}^{\infty} \left(\alpha_n . cos\left(\frac{2.\pi.n.t}{T}\right) + b_n . sin\left(\frac{2.\pi.n.t}{T}\right)\right), \tag{4.4}$$

where t is time, T is period, a_o, a_n and b_n components are defined by the Equation 4.5, Equation 4.6, Equation 4.7 such as

$$a_o = \left(\frac{2}{T}\right) \int_o^T x(t).dt, \tag{4.5}$$

$$a_n = \left(\frac{2}{T}\right) \int_o^T x(t).cos\left(\frac{2.\pi.n.t}{T}\right).dt, \tag{4.6}$$

$$b_n = \left(\frac{2}{T}\right) \int_o^T x(t).sin\left(\frac{2.\pi.n.t}{T}\right).dt, \tag{4.7}$$

As data of interest is obtained in digital format instead of analog format, a discretized form of Fourier series is more comprehensive for computational purposes. In case of discretization of signal within a finite time interval, representation of such function considering N number of time step is evaluated such as in the Equation 4.8

$$x(t_k) = \frac{a_o}{2} + \sum_{n=1}^{N/2} \left(a_n . cos\left(\frac{2.\pi.n.k}{N}\right) + b_n . sin\left(\frac{2\pi.n.k}{N}\right)\right), \tag{4.8}$$

where a_o ,a_n and b_n components are defined by the Equation 4.9, Equation 4.10 Equation 4.11 such as

$$a_o = \left(\frac{2}{N}\right).\sum_{k=1}^{N} X_k, \tag{4.9}$$

$$a_n = \left(\frac{1}{N}\right).\sum_{k=1}^{N} X_k.cos\left(\frac{2.\pi.n.k}{K}\right), \tag{4.10}$$

$$a_n = \left(\frac{1}{N}\right).\sum_{k=1}^{N} X_k.sin\left(\frac{2.\pi.n.k}{K}\right), \tag{4.11}$$

4.2.2. Signals in Frequency Domain

An alternative form of Fourier series could be evaluated by the Equation 4.12 including complex terms such as

$$x(t_k) = \frac{a_o}{2} + \sum_{n=1}^{N-1} X_n.e^{2.\pi.i.n.k/N}, \tag{4.12}$$

which makes discrete Fourier transform possible to convert such equation from time domain to frequency domain. As a result, the Equation 4.13 presents the data in the transformed domain.

$$X_n = \frac{1}{N} + \sum_{N}^{k=1} x_k.e^{-2.\pi.i.n.k/N}, \tag{4.13}$$

4.2.3. Cross Power Spectral Density

Power spectral density is representation of spectral values of a signal as a function of frequency. It is defined with units of g^2/Hz. The power term refers to the

square value of spectral density of a signal. Power spectral density received from an output refers to the response of the structure, under a certain type of dynamic loading. In other words, such response contains frequency domain information due to forcing function reflecting the excitation content, as well as the structural behaviour. In case of white noise excitations, input ground motions with low amplitude and broad band frequency content, forcing function is not expected to interfere in response signal with any predominant frequency. Therefore, power spectral density directly provides structural response. In contrast, earthquake excitations with high amplitude and narrow band frequency content does not result in a constant forcing function, but a function characterized by predominant frequencies of the excitation. In order to cancel out the effect of forcing function from response, response function should be divided by forcing function to obtain power spectral density in terms of pure structural terms such as in the Equation 4.14

$$H(w) = \frac{X}{F}, \tag{4.14}$$

where $H(w)$ is frequency response function, X is response function, F is forcing function.

In this way, two output signals could be utilized by cross power spectral density to eliminate non-structural response in frequency domain.

4.2.4. Problems in Digital Signal Processing

Measurements used in the study are composed of digital data converted from analog data. The distinction between these two types of data is that digital data is a discretized form of continuous analog data. Sorts of problems and misleading analysis results may arise in the absence of necessary signal processing treatments. Some of these problems are discussed and considered for better processing of acceleration data.

4.2.4.1. Aliasing. Conversion of analog signals to digital signals may cause aliasing in case inadequate sampling rate may cause misinterpretation of high frequency signals. In other words, discretization of signal leads losing data which is critical for detecting wave characteristics. Inability of processing the data properly could result in erroneous results in system identification. In this study, such problem is not expected as the sampling frequency is significantly high. The sampling frequency used in this study is 200 Hertz which make it possible to cover signals up to half of sampling frequency, 100 Hz. In structural and earthquake engineering, low frequency bands are of importance for revealing vibration characteristics of structures. For example, even the third mode of vibration analyzed in this study falls below 15 Hertz, showing that sampling rate is sufficiently high. Therefore, such problem is not observed in this study (Ewins, 2000).

4.2.4.2. Leakage. Non-periodicity of the signal within the finite time interval of observation could cause leakage of energy in terms of spectrum. In other words, a signal characterized by a single and specific frequency could be represented with a frequency band which reduces the performance of signal processing and deterioration in the actual spectrum. This problem could be avoided by applying windowing techniques to the signal (Ewins, 2000).

4.2.4.3. Windowing. Windowing emerges to prevent leakage problem. As it is mentioned, such problem arises from the non-periodicity, and windowing forces the signal to be modified into a periodical state within the given finite time interval. Such modification is enabled by multiplication of non-periodic signal with periodic windowing function (Ewins, 2000).

4.2.4.4. Averaging. The need for averaging process stems from inadequacy of Fourier transform in case of analysis of random vibrations. Averaging process attempts to improve statistical reliability, and decrease the effect of random noise in the signal. By taking Fourier transform in short time intervals, then overlapping and averaging within these intervals, random noise removal can be possible (Ewins, 2000).

4.2.4.5. Filtering. During the recording of a signal, many sort of environmental or operational factors could be the sources of noise in signal. Noise could be produced from electrical devices composing the data recording system as well as external factors. As a result, signal characteristics could involve components that stems from sources other than structural response. It is essential to remove the majority of such noise so that structural effects could be much widely comprehended. The high frequency and transient noise could be avoided by applying low-pass filters. Slight shifts observed in the time domain of the signal refers to very low frequency noise which could be prevented as well. After applying filtering, pure structural characteristics could be evaluated efficiently (Ewins, 2000).

4.3. Frequency Domain Identification

System identification in frequency domain involves two main steps such as identification of modal values and structural parameter identification based on finite element model updating.

4.3.1. Frequency Domain Decomposition

A frequency domain decomposition (FDD) technique developed by Brincker *et al.*, (2001) attempts to extract modal parameters without the input information. A number of outputs transformed into frequency domain compose a series of square matrices. The dimension of these square matrices are the number of outputs. Furthermore, the number of square matrices depend on the length and discretization of the frequency domain. Accordingly, a three dimensional matrix is formed such as $A(i, j, k)$ where an element denoted by such dimension refer to the cross power spectral density of ith output with respect to jth output in the kth step of frequency domain. Singular value decompositon of the square matrix at kth frequency returns the spectral value and the mode shape at such frequency. Decomposition of spectral density matrix is done as in the Equation 4.15.

$$S_{YY}(w) = U(w).\sum(w).U^H(w), \tag{4.15}$$

where $\sum(w)$= diagonal matrix of the singular values, $U(w)$=unitary matrix of the singular vectors. and the superscript H denotes the complex conjugate and transpose.

Spectral values could be connected to illustrate the response of outputs in frequency domain. In this way, close modes could be extracted by such fine discretization of frequency domain and modal frequencies could be accurately detected. Afterwards, mode shapes corresponding to the identified modal frequencies could be detected. Therefore, in spite of existence of closed and damped modes, extraction of modal parameters with high accuracy could be accomplished with an output only method.

In Figure 4.1, power spectra of WN1, WN2, WN3, and WN4 obtained from FDD method is illustrated. According to that, damage progression could be tracked by the shift of peak frequencies to the left. In other words, as expected, decrease in structural stiffness results in a decrease in modal frequencies. Such phenomena could be simply supported with the Equation 4.16 which is the solution of differential equation of motion corresponding to a single degree of freedom system (Chopra, 2007).

$$f_n = \frac{\sqrt{\frac{k}{m}}}{2.\pi}, \tag{4.16}$$

where f_n is natural frequency of vibration, k is stiffness, m is mass.

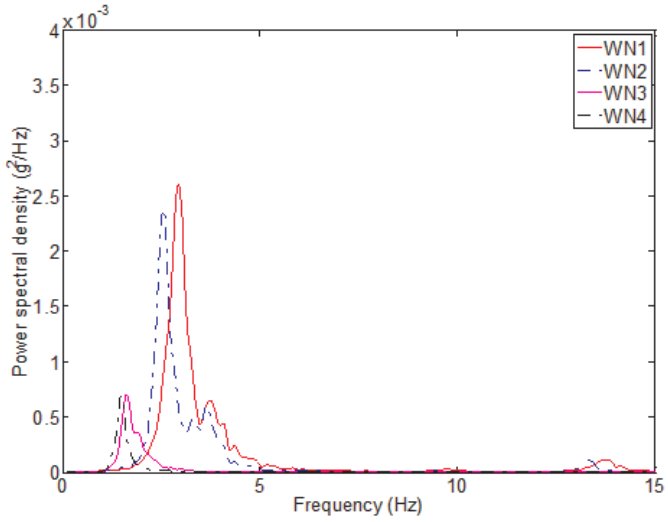

Figure 4.1. Modal frequencies obtained from responses to white-noise inputs.

4.3.2. Error Minimization and Finite Element Model Updating

Modal analysis is applied to each candidate finite element model with a specific combination of bent stiffness parameters. As a result, eigenvalues and eigenvectors of the model is obtained. Eigenvalues and eigenvectors correspond to the modal frequencies and mode shapes of the model, respectively. These modal parameters constitute the simulated model's contribution into the error function. Likewise, error function includes measured modal parameters which are based on application of FDD to acceleration signals obtained from output data. In addition, error function considers not only modal parameters but also their confidence levels. Generally, evaluation of such confidence level is interpreted in terms of multiplication of weighing factor and error caused by corresponding modal parameter. These modal parameters are errors resulting from modal frequencies and mode shapes. Consideration of error due to modal frequency of a certain mode is in percentage such as the difference between measured and simulated modal frequency, divided by measured modal frequency. Square value of this difference is taken to obtain the error in positive terms. Similarly, error due to mode shapes are characterized by the difference between measured and simulated mode shapes. Such difference is evaluated with the help of modal assurance criteria (MAC) expressed in the Equation 4.17.

$$MAC = \frac{|\psi_*^T.\psi|^2}{(\psi_*^T.\psi_*).(\psi^T.\psi)}, \tag{4.17}$$

where ψ_* is the measured mode shape, ψ is the simulated mode shape of corresponding mode.

And the superscript T denotes the transpose.

As MAC value approaches 1, the correlation between measured and simulated mode increases. Therefore, obtained MAC value is substracted from 1 to interpret such value in terms of error. Square of such error is taken to use the same order with the error sourced from modal frequency terms.

Evaluation of confidence level and weighing factors of any modal parameter is open to discussion. The reasonable approach is to favor primary modes of vibration because of their dominant influence on vibration characteristics. Accordingly, the first, second, and third modal frequencies are taken into consideration as well as the first mode shape. Therefore, weighing coefficients of such modal parameters is set to 1, while other parameters' coefficients are set to 0. Eventually, error as a function of bent stiffness values is defined with the Equation 4.18

$$E(\alpha_1, \alpha_2, \alpha_3) = \sum_{i=1}^{3} (k_i.[(f_i^* - f_i)/f_i^*]^2 + h_i.[1 - MAC_i]^2), \tag{4.18}$$

where $\alpha_1, \alpha_2, \alpha_3$ are bent stiffness modification factor of bent 1, bent 2, bent 3, respectively, i is mode number, k_i is weighing coefficient for ith modal frequency, h_i is weighing coefficient for ith MAC value, f_i^* is measured modal frequency of ith mode, f_i is simulated modal frequency of ith mode, MAC_i is modal assurance criteria for ith mode shape.

In other words, k_1,k_2, k_3 and h_1 is set to 1 and other coefficients are set to 0. For the initial conditions, referring to damage state 1 or WN1, error curve is plotted as a function of stiffness coefficient of all bents in the Figure 4.6. It is illustrated that error function is minimized at the stiffness value of 0.5. In this way, bent stiffness values are identified for state-1.

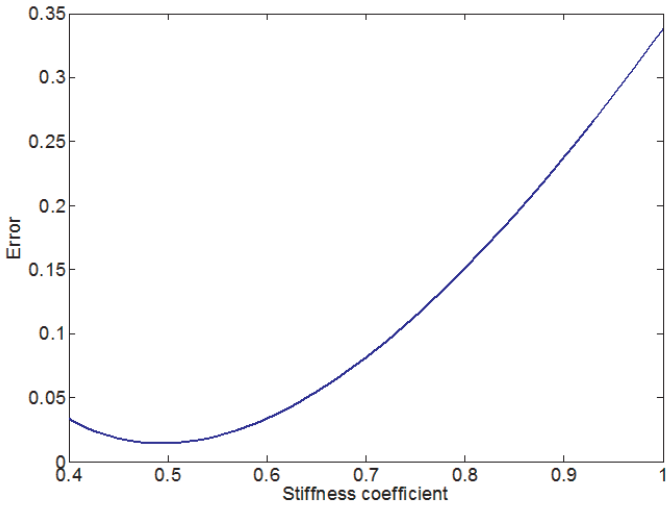

Figure 4.2. Error curve of frequency domain identification of WN1.

Following the procedure described above, modal frequencies and mode shapes are identified, resulting in finite element model updating at each state. Table 4.1, Table 4.2, Table 4.3 and Table 4.4 show the updated and non-updated modal frequencies,while Figure 4.3, Figure 4.4, Figure 4.5 and Figure 4.6 show the updated and nonupdated mode shapes corresponding to state-1, state-2, state-3, and state-4, respectively. Table 4.1 reveals that finite element model updating significantly decreases the error due to simulated modal frequencies. Such decreases in errors are from 35.6% to 2.7% for the first mode, and from 45.6% to 4.6% for the second mode. Even though the error in third mode increases, its effectiveness in vibrational characteristics is negligible compared with the first modes. For the remaining states, such increase in accuracy could be observed as well. Therefore, the validity of identification is verified by the results presented in the Table 4.1, Table 4.2, Table 4.3 and Table 4.4.

Table 4.1. Modal Frequencies from Measurement and FEM (WN1).

	target (measured)	initial (nonupdated)	Δf	updated	Δf
f_1	2.98	4.04	35.6 %	2.90	2.7 %
f_2	3.66	5.33	45.6 %	3.83	4.6 %
f_3	13.87	13.07	5.8 %	12.4	10.6 %

Table 4.2. Modal Frequencies from Measurement and FEM (WN2).

	target (measured)	initial (nonupdated)	Δf	updated	Δf
f_1	2.59	2.90	12.0 %	2.63	1.5 %
f_3	3.66	3.83	4.7 %	3.67	0.3 %
f_3	13.33	12.4	7.0 %	12.33	7.5 %

Table 4.3. Modal Frequencies from Measurement and FEM (WN3).

	target (measured)	initial (nonupdated)	Δf	updated	Δf
f_1	1.66	2.63	58.4 %	1.66	0.0 %
f_2	1.9	3.67	93.2 %	1.93	1.6 %
f_3	13.13	12.33	6.1 %	11.93	9.1 %

Table 4.4. Modal Frequencies from Measurement and FEM (WN4).

	target (measured)	initial (nonupdated)	Δf	updated	Δf
f_1	1.51	1.66	9.9 %	1.45	4.0 %
f_2	1.61	1.93	19.9 %	1.56	3.1 %
f_3	12.89	11.93	7.5 %	11.89	7.8 %

In Figure 4.3, Figure 4.4, Figure 4.5 and Figure 4.6, measured and simulated (finite element model updated) mode shapes are illustrated. In Figure 4.3, the first, and third simulated mode shapes are in very good correlation with mode shape obtained from FDD. Although as not accurate as first and third mode, second mode shape also agrees with measured mode shape. Such statements are also valid for other damage states.

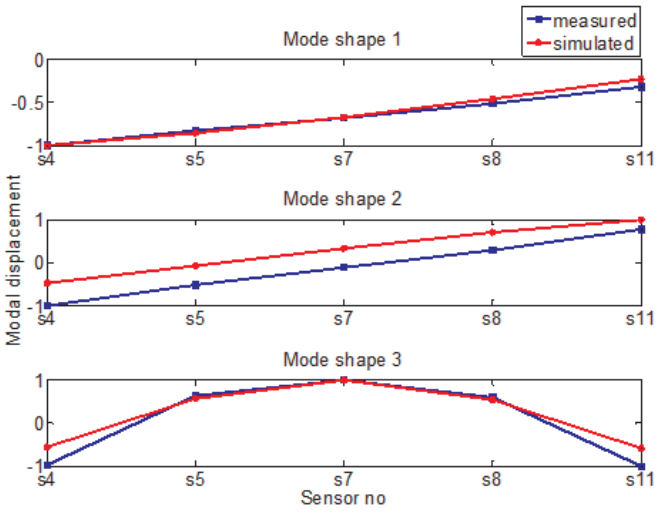

Figure 4.3. Modal shapes from measurement and FEM (WN1).

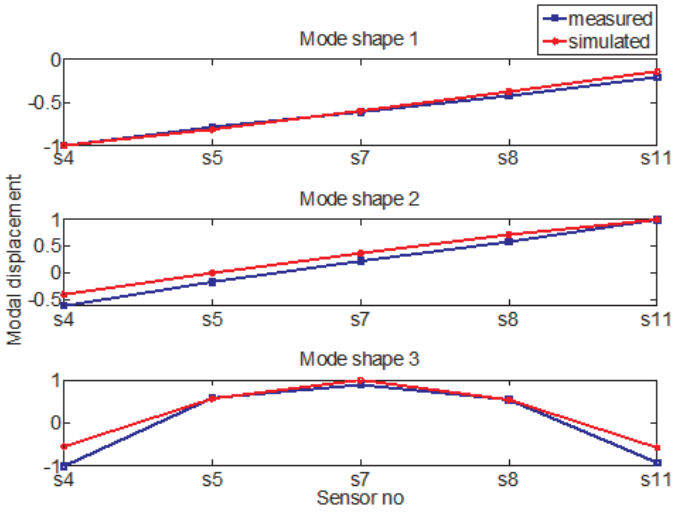

Figure 4.4. Modal shapes from measurement and FEM (WN2).

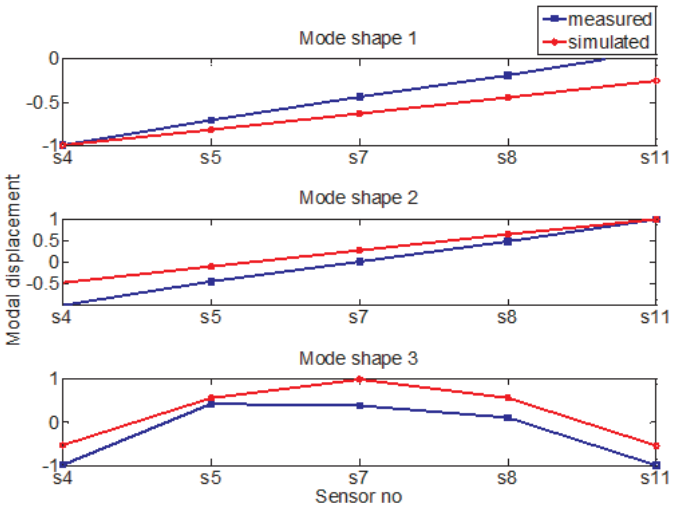

Figure 4.5. Modal shapes from measurement and FEM (WN3).

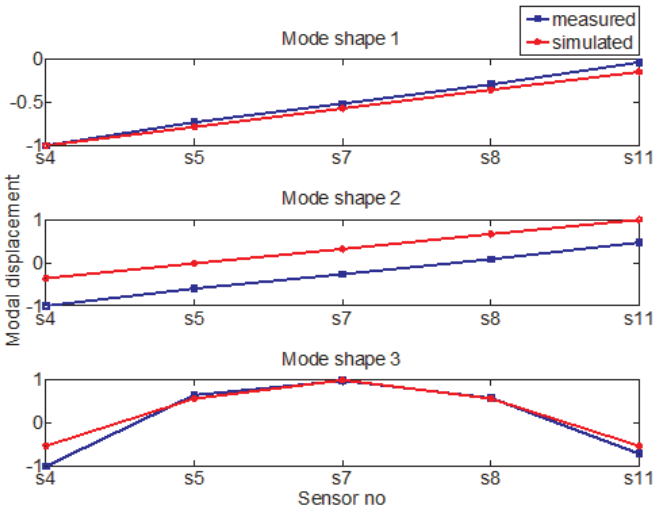

Figure 4.6. Modal shapes from measurement and FEM (WN4).

Consequently, it is concluded that structural system identification and finite element model updating in frequency domain enables to decrease the error between measured and simulated modal parameters to a great extent, hence, provides accurate models for reliability estimation.

4.4. Time Domain Identification

4.4.1. Linear Time History Analysis

Base finite element model is developed in OpenSees platform for linear time history analysis. Deck, bent beams, and columns are assigned as elastic beam column elements. The additional, and discretized self-weight masses are assigned proper with their actual locations. In order to take the difference in measured input motions of different shaking tables into consideration, excitation is modeled as multiple support excitation rather than uniform excitation. Figure 4.7 presents the slight difference between measured ground motion inputs of bent-1 (sensor 1), bent-2 (sensor 6), and bent-3 (sensor 9), during WN1 excitation.

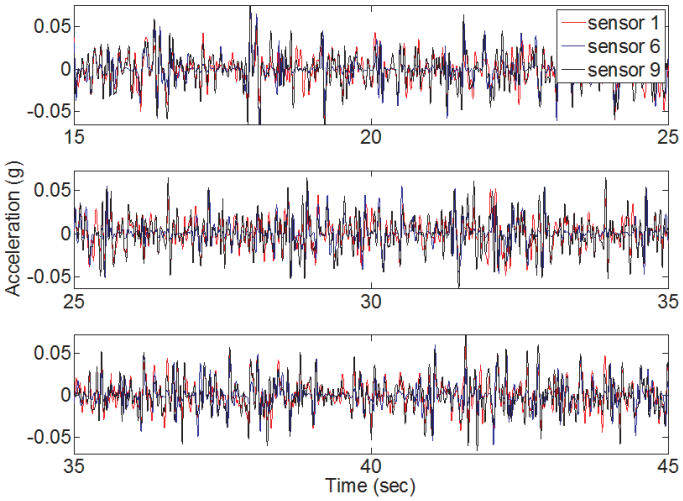

Figure 4.7. Measured input ground motions from bent-1, bent-2, and bent-3 (WN1).

Multi-support excitation analysis requires input ground motions in terms of displacement rather than acceleration. Therefore, double integration of acceleration data into displacement data is required. Even though OpenSees provides such integration tool as a built-in function, baseline correction of such data is not applicable. Therefore, it is recommended to proceed double integration procedure manually. Accordingly, integration of acceleration data into velocity is completed with the baseline correction of velocity data. Similarly, second integration is completed, and displacement data with

no baseline shift is produced. Finally, time history analysis is conducted and analysis results are interpreted to evaluate error between simulation and measurement. It should be noted that uniform excitation analysis provides acceleration response in terms of relative values, whereas multi-support excitation provides acceleration response in terms of absolute values. For this reason, simulated response obtained from multi-support excitation can be directly compared with the measured response, whereas uniform excitation requires subtraction of ground motion input from simulated outputs.

4.4.2. Error Minimization and Finite Element Model Updating

Time domain identification is based on evaluating the error between measured and simulated values by least-square method (Ljung, 1999). The measured and simulated data consists of acceleration time histories of output points. The measured acceleration time histories are the recorded outputs of accelerometers. Similarly, time history analysis of finite element model and extraction of acceleration from output nodes refer to the simulated acceleration time histories. Only the data proper with location of sensor 4, 7 and 11 is taken into consideration, as they provide responses on top of bent-1, bent-2, and bent-3, respectively. Error due to each time step, which is subtraction of simulated acceleration from measured acceleration, contributed with its square value; and summed up as a single error representing a single candidate finite element model. As in the frequency domain error minimization, each candidate finite element model represents a combination of bent stiffness values, but with initiation of a new parameter, damping ratio, ξ. Consequently error function in time domain is defined by the Equation 4.18

$$E(\alpha_1, \alpha_2, \alpha_3, \xi) = \sum_{i=1}^{3} \Big(\sum_{j=1}^{n} \Big[a_{ij}^{*} - a_{ij} \Big]^2 \Big), \tag{4.19}$$

where i is node number, n is time step of measured acceleration, a_{ij}^{*} is measured acceleration at ith node at jth time step, a_{ij} is simulated acceleration at ith node at jth time step.

Figure 4.8 illustrates the error surface of WN1 excitation. It is observed that

the error is minimized at the damping ratio of 0.05 and the stiffness coefficient of 0.6. Furthermore, it is seen that error function is more sensitive to damping ratio than stiffness coefficients. The proceeding damage states are identified with a similar approach.

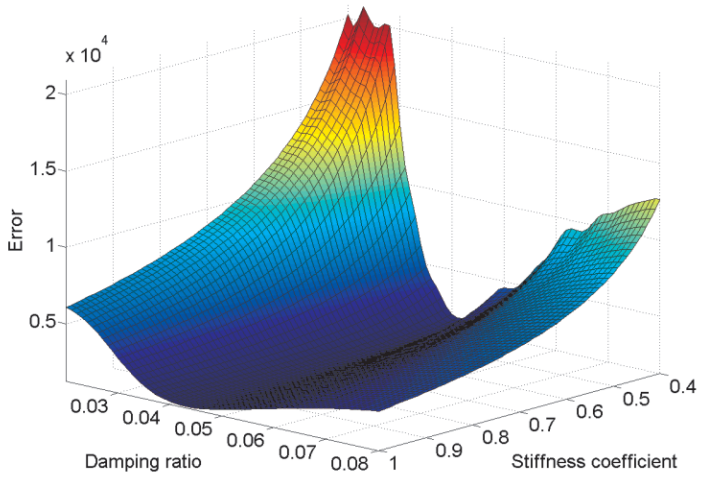

Figure 4.8. Error surface of time domain identification of WN1.

Figure 4.9 show the time history outputs of measured, non-updated and updated responses. It includes acceleration data regarding sensor 4, 7 and 11 which reflect responses on top of bent-1, bent-2, and bent-3, respectively. It is conclusive that finite element model updating in time domain significantly reduces the error between measured and simulated response. The correlation between updated response and measured response is very significant, in contrast with non-updated model's poor performance. Likewise, Figure 4.10, Figure 4.11 and Figure 4.12 shows the time history outputs of WN2, WN3, and WN4 excitations, respectively. These results also provide evidence for increasing correlation between measured and simulated response due to finite element model updating.

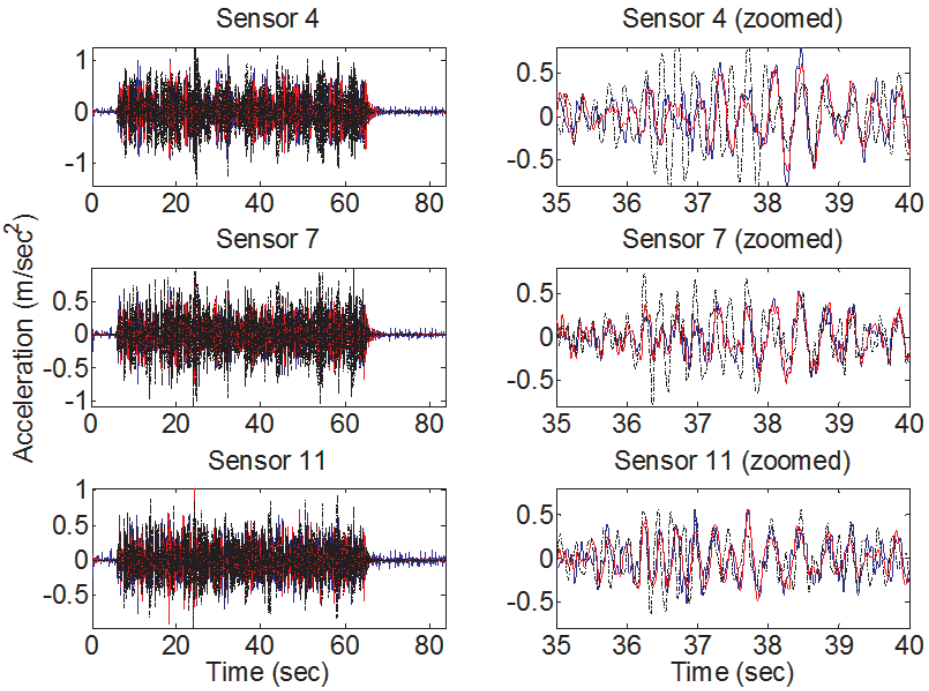

Figure 4.9. Measured and simulated time histories under WN1.

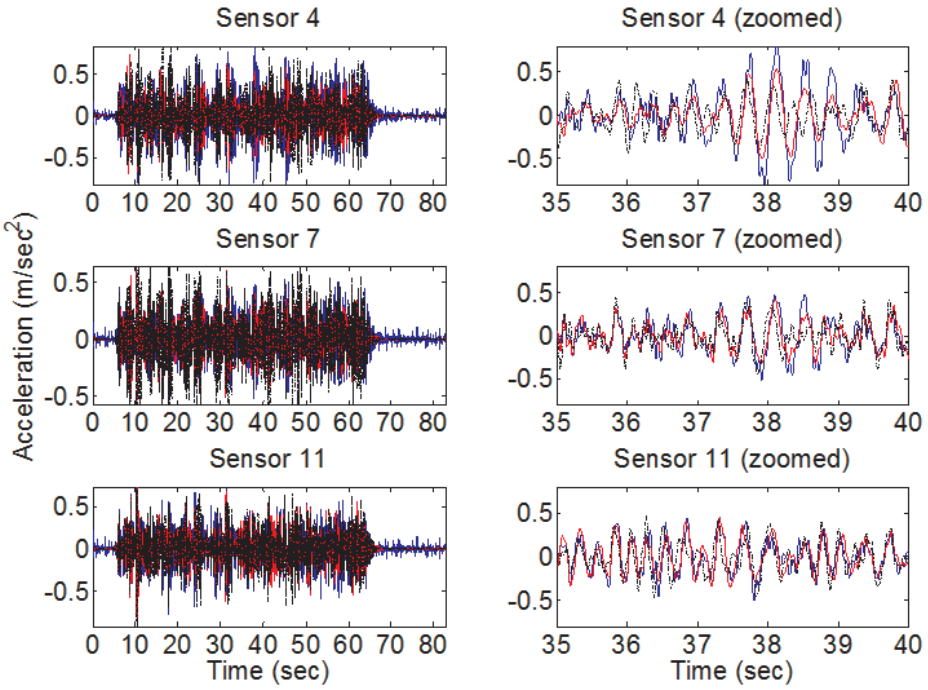

Figure 4.10. Measured and simulated time histories under WN2.

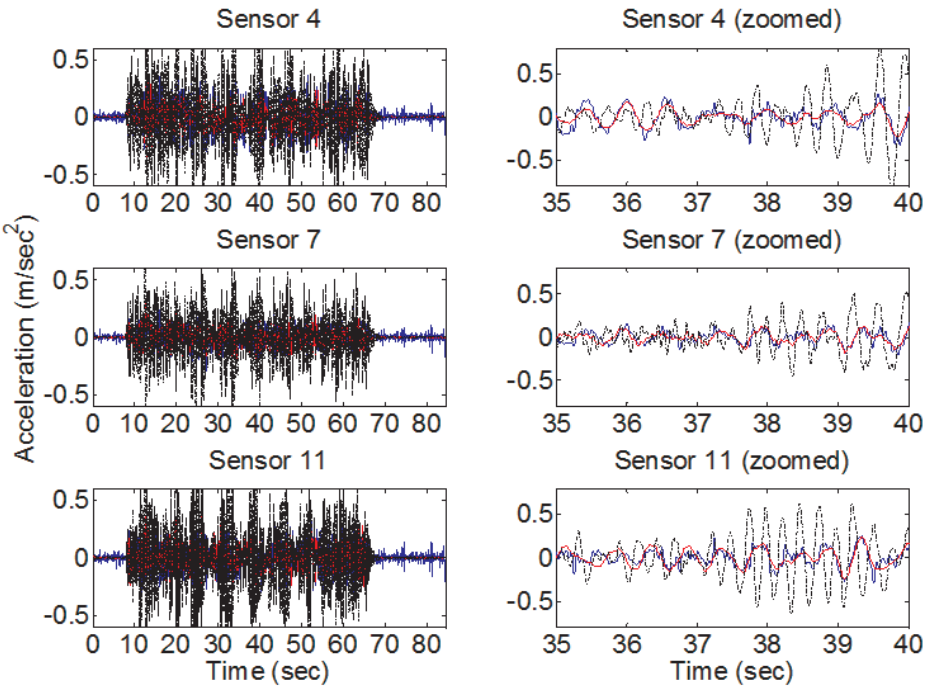

Figure 4.11. Measured and simulated time histories under WN3.

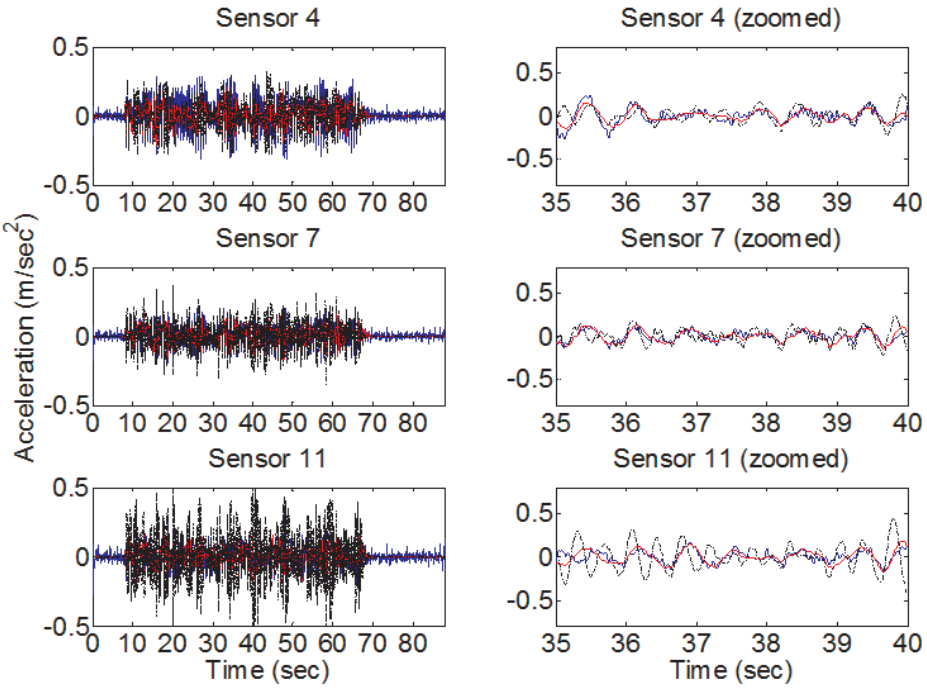

Figure 4.12. Measured and simulated time histories under WN4.

5. NONLINEAR TIME HISTORY ANALYSIS

5.1. General

Nonlinear time history analyses are carried out to estimate post-event damage state of the structure with the pre-event damage information and known input ground motion. Such procedure is followed as an alternative for system identification and finite element model updating to determine the damage level of structural members at a certain state.

In order to run a nonlinear time history analysis, the type of nonlinearity should be determined. In this context, representation of nonlinear behaviour with concentrated or distributed plasticity is influential as well as consideration of stiffness and strength degradation. Furthermore, the level of nonlinearity; whether it is observed on fiber, section, member or structure; plays an important role in accuracy and sensitivity of analysis (Yazgan and Dazio, 2011).

5.2. Generation of Rotational Springs

In reinforced concrete structures, rotation at column ends is a robust measure for damage indication. Therefore, in this study, concentrated nonlinearity at column end regions is taken into consideration by modelling rotational springs at the upper and lower column end regions. These rotational springs are characterized by elastic-perfectly plastic moment-curvature relationship. This relationship is idealized based on an original sectional moment-curvature relationship which is obtained using Response-2000 sectional analysis program developed by Bentz and Collins (2000). Idealization parameters such as yielding moment and curvature are determined proper with the approach proposed by (Gardoni *et al.*, 2002) seen in Figure 5.1.

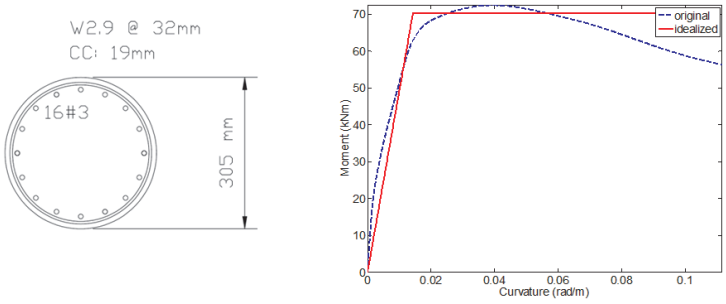

Figure 5.1. Cross-sectional properties and moment-curvature relationship of columns.

The relationship between yield curvature and yield rotation could be defined by the Equation 5.1 such as

$$K_y = \frac{\theta_y}{L_p}, \tag{5.1}$$

where K_y is yield curvature, θ_y is yield rotation, L_p is plastic hinge length.

Furthermore, initial stiffness could be expressed in terms of moment and curvature as in the Equation 5.2

$$EI = \frac{M}{K}, \tag{5.2}$$

where EI is initial stiffness, M is moment, K is curvature.

5.3. Evaluation of Post-Event Stiffness and System Damping Ratio

Effective stiffness could be derived by obtaining ductility and initial stiffness proper with the Equation 5.3 mentioned by (Priestley *et al.*, 1996).

$$EI_{eff} = \frac{EI}{\mu}, \tag{5.3}$$

where EI_{eff} is effective stiffness, μ is ductility.

To summarize, stiffness of the damaged region and primary slope of moment-rotation relationship is inversely proportional with ductility; which is an expression of structural damage due to earthquake excitations.

Another chief structural parameter, damping ratio could be estimated after damaging event in terms of ductility such as (Kowalsky 2002) with the Equation 5.4.

$$\xi_{eff} = 0.05 + \frac{1}{\pi}.\left(1 - \frac{0.95}{\sqrt{\mu}} - 0.05.\sqrt{\mu}\right), \tag{5.4}$$

where ξ_{eff} is the equivalent damping ratio.

At this level, damping ratio specifically refers to an individual structural member. Such definition should be enhanced in order to represent the overall structural behaviour. Accordingly, equivalent damping values obtained from each member are evaluated to determine system damping matrix. In this case, each member's contribution is proportional with column drift ratios, which are represented with a weighing factor such as in the Equation 5.5.

$$Q_i = \frac{\Delta_i}{L_i}, \tag{5.5}$$

where Q_i is the weighing factor for the ith column, Δ_i is the displacement quantity associated with the ith column, L_i is the ith column length.

Finally, damping ratio, with a reduction from member level to structural level, could be determined with the Equation 5.6 such as

$$\xi_{sys} = \Sigma_i\left(\frac{Q_i}{\Sigma Q_i}.\xi_i\right), \tag{5.6}$$

where ξ_{sys} is system damping ratio.

Given the input ground motion, such nonlinear dynamic analysis procedure could be used to simulate changes in structural parameters due to structural damage in terms

of ductility.

5.4. Nonlinear Dynamic Analysis Results

Nonlinear finite element model is developed in OpenSees platform proper with Mazzoni *et al.*, (2007). Deck elements, bent beam elements, excitation types and other properties are defined as in the linear model. Column members are seperated into three regions where lower and upper regions represent plastic hinge regions. Lower and upper regions of columns are connected to middle regions by rotational springs based on the previous discussions. The initial state involves identification of column stiffness where no damage has initiated into the structural system. Therefore, column stiffness modification factors modify all of these regions. For the following states, the states structural system experiences damage, stiffness modification factors affected only lower and upper regions where damage is expected due to plastic hinge formation. Rotational springs are assigned by the bilinear hysteretic model elements with a zero secondary stiffness to entail elastic-perfectly plastic moment-curvature relationship.

Nonlinear time history analysis is conducted for each damaging event, and ductility values of rotational hinges are obtained in terms of rotation. Pre-event stiffness of lower-upper end regions are modified reversely proportional with such ductility values to produce post-event stiffness values. Moment-curvature behaviour is modified in conjunction with such procedure. Sequentially, post-event values of ith nonlinear time history analysis becomes pre-event values of $(i+1)$th nonlinear time history analysis. Figure 5.2, Figure 5.3 and Figure 5.4 shows moment-rotational response of rotational hinges located at bent-1, bent-2, and bent-3, respectively. According to nonlinear time history analysis results, it is shown that at the end of T14, bent-1 experienced the highest damage such as 1.29 of ductility, whereas insignificant damage is observed on bent-3, and no damage is observed on bent-2. This is compatible with observations and identification results. Accordingly, ductility values of bent-1, bent-2, bent-3 are 5.27, 2.15, 4.86 at the end of T17, and 8.95, 9.45, 18.39 at the end of T19, respectively.

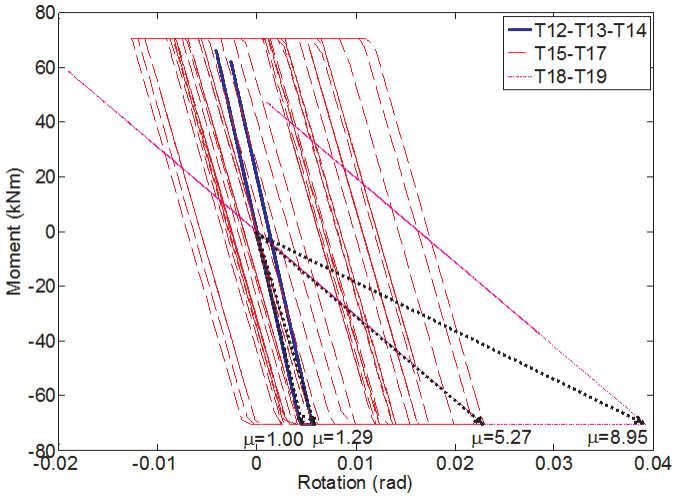

Figure 5.2. Moment-rotation response of bent-1.

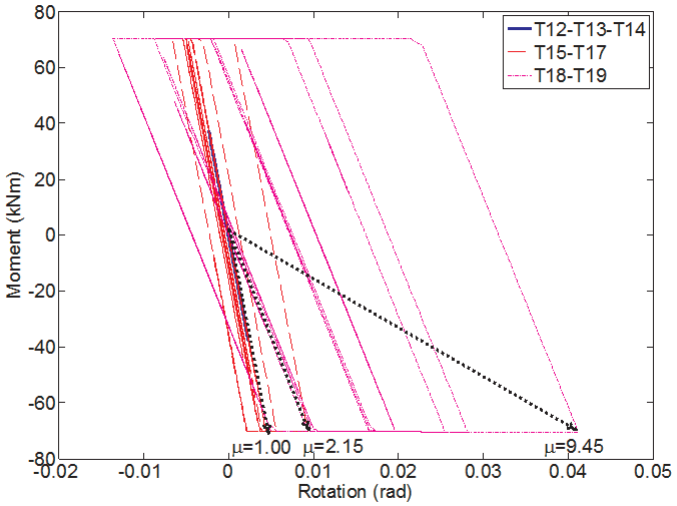

Figure 5.3. Moment-rotation response of bent-2.

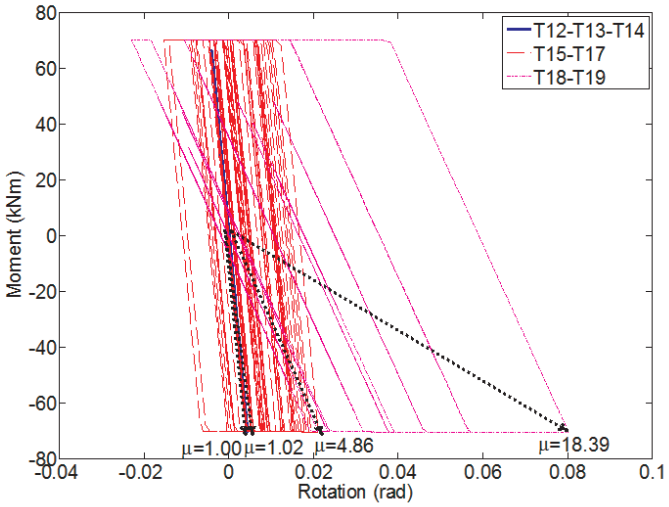

Figure 5.4. Moment-rotation response of bent-3.

Based on ith nonlinear time history analysis, system damping is obtained as a function of ductility demands of columns. As a result, such post-event damping ratio estimation is assigned as pre-event damping ratio of $(i+1)$th nonlinear time history analysis, and the following damping ratios are evaluated similarly.Table 5.1 shows the estimations of system damping based on nonlinear time history analysis results.

Table 5.1. System Damping Calculations.

State	ductility			Equivalent Damping			Q			System Damping
	B1	B2	B3	B1	B2	B3	B1	B2	B3	
1	-	-	-	-	-	-	-	-	-	
2	1.29	1.00	1.02	0.084	0.050	0.052	0.069	0.036	0.019	0.0681
3	5.27	2.15	4.86	0.200	0.139	0.196	0.070	0.036	0.019	0.1826
4	8.95	9.42	18.36	0.220	0.221	0.230	0.072	0.034	0.021	0.222

6. IDENTIFIED AND PREDICTED DAMAGE PROGRESS

6.1. Overview

In this section, an overview of the change in identified and predicted parameters, namely, bent stiffness values and damping ratios, with damage progress is presented. Besides, parameters originating from system identification and nonlinear time history analysis are compared. Such parameters are investigated with a classification of two groups such as identified/updated and predicted/non-updated approaches. Structural system identification and finite element model updating constitutes the identified approach, whereas damage prediction based on nonlinear time history analysis points out the predicted approach. Eventually, both groups attempt to evaluate modification factors for structural parameters. Damage state 1, 2, 3, and 4 presented in this section refers to the states during white noise excitations of WN1, WN2, WN3, WN4 or states before and after earthquake excitations of T12-T13-T14, T15-T17, T18-T19, respectively. White noise and earthquake excitation measurements are used for generation of updated and non-updated parameters, respectively.

Identified approach involves identification of bent stiffness values both in time and frequency domain, but damping ratio identification is not carried out in frequency domain. Generation of non-updated parameters is initialized with 5% damping ratio, and cracked EI values based on ACI 318-08 provisions (2008) which refers to the 0.7 of original EI values. Stiffness values at the later states are obtained by determining effective stiffness due to nonlinear time history analysis. Likewise, damping-ductility relationship equations are used to determine post-event damping ratio due to nonlinear time history analysis.

6.2. Damage Progress in terms of Bent Stiffness Values

It is shown in Figure 6.1 that there is a correlation between identified stiffness values in frequency and time domain. Moreover, in spite of the similar trend between updated and non-updated stiffness value, the difference between these two values are visible. For the first and second states, non-updated stiffness values are significantly higher than updated stiffness values. For instance, due to T12-T13-T14, bent-3 is exposed to significant damage according to identified parameters. Time domain identification and frequency domain identification indicates a reduce from 0.6 to 0.36 and from 0.5 to 0.35, respectively. Unlikely, predicted parameter is almost incapable of damage indication. Such difference between identified and predicted parameters reduces in the third and fourth damage states.

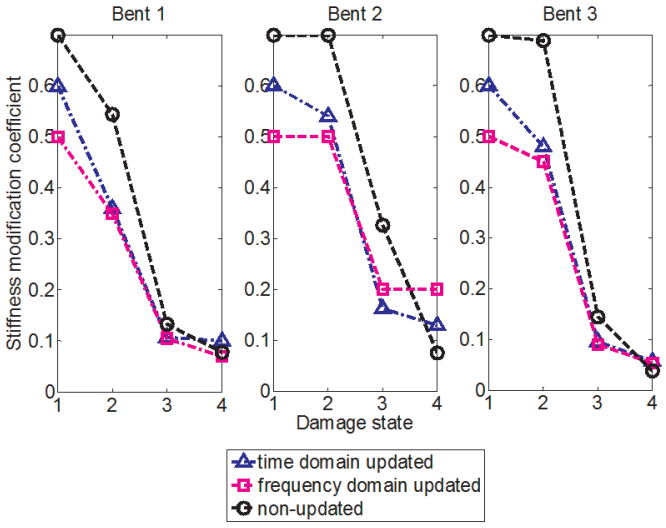

Figure 6.1. Stiffness values at different damage levels.

6.3. Damage Progress in terms of Damping Values

Damping ratio, either identified or predicted, corresponds to the viscous damping ratio. Table 6.1 compares identified and predicted damping ratio changing with damage state. One of the outcomes is that damage progression results in an increase in damping ratio. Another observation is the increasing gap between identified and predicted damping ratio with damage progression. Especially in the third and fourth

damaged states, system damping estimation of predicted model reaches extreme values such as 18%, and 22%, respectively. In contrast, identified damping ratios follow a smoother path compared with predicted damping ratios.

Table 6.1. Damping ratio values at different damage levels.

State	Updated/ Non-updated	System Damping
1	U	0.050
	N	0.050
2	U	0.060
	N	0.068
3	U	0.096
	N	0.183
4	U	0.115
	N	0.222

To summarize, finite element models are modified according to the identification and prediction results. These modification procedure include bent stiffness values, moment-curvature relationships of plastic hinge sections, and damping ratios. Using modified finite element models of different states and approaches, structural reliability estimations are carried out.

7. RELIABILITY ESTIMATION

7.1. Introduction

Structural reliability estimation is of great importance for structural health monitoring as it offers a prospective future for the ultimate goal of structural health monitoring, residual life assessment. Furthermore, it provides valuable and practical information for crisis management and hazard mitigation strategies. In other words, its contributions are beneficial for communication of structural and earthquake engineering with related disciplines, local authorities and decision makers.

It has been discussed that structural system identification reflects the global dynamic characteristics of structure measured with the use of sensors and data acquision equipments. Such information is priceless for understanding the actual structural behaviour, as pure analytical approaches may include extensive misleading assumptions. Therefore in this study, a thorough methodology, which investigates all available analytical and experimental data, and integrates reliability estimation and system identification, is diligently attempted. Combining two distinct subjects, reliability estimation and system identification, residual life assessment could be anticipated with an advanced and accurate approach.

In this study, fragility curves are generated for reliability estimation. Many different sources of uncertainty may exist arising from load, material and system modelling of structures. Within the context of this study, earthquake loads are considered as the primary source of uncertainty. Therefore, earthquake excitation is designated as the random variable by one of the main strong ground motion parameters, peak ground acceleration (PGA). Comprehensive information regarding structural reliability estimation can be found in (Melchers, 1999), (Ang and Tang, 1975), (Ang and Tang, 1984).

7.2. Methodology

A fragility curve is a cumulative probability density function which attempts to fit a set of failure probability data each pointing a specific PGA. The error minimization between fragility curve and corresponding data set is handled by maximum likelihood estimation. The curve is basically defined with two parameters such as mean and standard deviation, which are to be obtained with the procedure explained below.

For the evaluation of probabilistic data sets, failure is defined as exceedence of a given threshold value. Accordingly, failure probability returns binary results, either 1 as threshold is exceeded or 0 otherwise. Such threshold value is interpreted in terms of ductility. Ductility demand for a specific ground motion is determined by the response due to nonlinear time history analysis. These ductility demands could be utilized to develop different fragility curves corresponding to different damage severities. The damage levels introduced by (Banerjee and Shinozuka, 2008) are used in this study, and shown in the Table 7.1.

Table 7.1. Rotational Ductility Limits.

Damage Level	Ductility Demand
No	$\mu < 1$
Almost No	$1 < \mu < 1.52$
Minor	$1.52 < \mu < 3.10$
Moderate	$3.10 < \mu < 5.72$
Major	$5.72 < \mu < 8.34$
Collapse	$8.34 < \mu$

In order to avoid intersection of fragility curves, the methodology should be able to ensure the dependence of probabilities at a given damage level. Therefore, formulation should bind the probability parameters together such as in Equation 7.1, Equation 7.2, Equation 7.3, Equation 7.4, Equation 7.5 and Equation 7.6

$$P_{i1} = 1 - F_1(a_i, c_1, \sigma), \tag{7.1}$$

$$P_{i2} = F_1(a_i, c_1, \sigma) - F_2(a_i, c_2, \sigma), \tag{7.2}$$

$$P_{i3} = F_2(a_i, c_2, \sigma) - F_3(a_i, c_3, \sigma), \tag{7.3}$$

$$P_{i4} = F_3(a_i, c_3, \sigma) - F_4(a_i, c_4, \sigma), \tag{7.4}$$

$$P_{i5} = F_4(a_i, c_4, \sigma) - F_5(a_i, c_5, \sigma), \tag{7.5}$$

$$P_{i6} = F_5(a_i, c_5, \sigma), \tag{7.6}$$

where c_1, c_2, c_3, c_4, c_5 are mean values of 1st, 2nd, 3rd, 4th and 5th fragility curves, σ is standard deviation of all fragility curves, a_i is the PGA of ith input ground motion, F_i is the cumulative probability density function, P_i is the failure probability.

1st, 2nd, 3rd, 4th and 5th fragility curves point out the exceedence of almost no, minor, moderate, major, collapse ductility demands, respectively. Using this probability formulation, likelihood estimation is conducted from Equation 7.7 such as

$$L(c_1, c_2, c_3, c_4, c_5, \sigma) = \prod_{i=1}^{151} \prod_{k=1}^{6} P(a_i, E_k)^{x_{ik}}, \tag{7.7}$$

where n is the number of dynamic analyses performed with different input ground motions, k is the number of fragilities (probabilities) evaluated at ith analysis (PGA), $x_{ik} = 1$ (if damage state E_k occurs for the ith analysis subjected to $a = a_i$), $x_{ik} = 0$ (if damage state E_k does not occur for the ith analysis subjected to $a = a_i$).

Equation 7.8 denotes extraction of mean values and standard deviation of fragility

curves from maximum likelihood estimation by the derivatives such as

$$\frac{\partial lnL(c_1,c_2,c_3,c_4,c_5,\sigma)}{\partial c_1} = \frac{\partial lnL(c_1,c_2,c_3,c_4,c_5,\sigma)}{\partial c_2} = \frac{\partial lnL(c_1,c_2,c_3,c_4,c_5,\sigma)}{\partial c_3} = \frac{\partial lnL(c_1,c_2,c_3,c_4,c_5,\sigma)}{\partial c_4} = \frac{\partial lnL(c_1,c_2,c_3,c_4,c_5,\sigma)}{\partial c_5} = \frac{\partial lnL(c_1,c_2,c_3,c_4,c_5,\sigma)}{\partial \sigma} = 0 \quad (7.8)$$

Such equation includes a great number of equations which needs computational effort to be solved. A built-in Matlab (2009) function, fminsearch, finds minimum of unconstrained multivariable functions using a derivative free method. Fminsearch function requires initial estimates for parameters of interest, which should be made with reasonable values. Otherwise, convergence problems may arise, and deceptive local minima values could entangle the estimations. Accordingly, such function is performed to find fragility curve parameters.

7.3. Development of Fragility Curves

In this study, 151 ground motion records of Northridge Earthquake (1994) are selected from Pacific Earthquake Engineering Center (PEER) database (2005). Figure 7.1 illustrates exemplary data sets and corresponding fragility curves of different ductility levels regarding the initial state, state 1, of non-updated model where no structural damage has introduced yet. Likewise, fragility curves of state 2, 3, and 4 is generated based on both of updated and non-updated models.

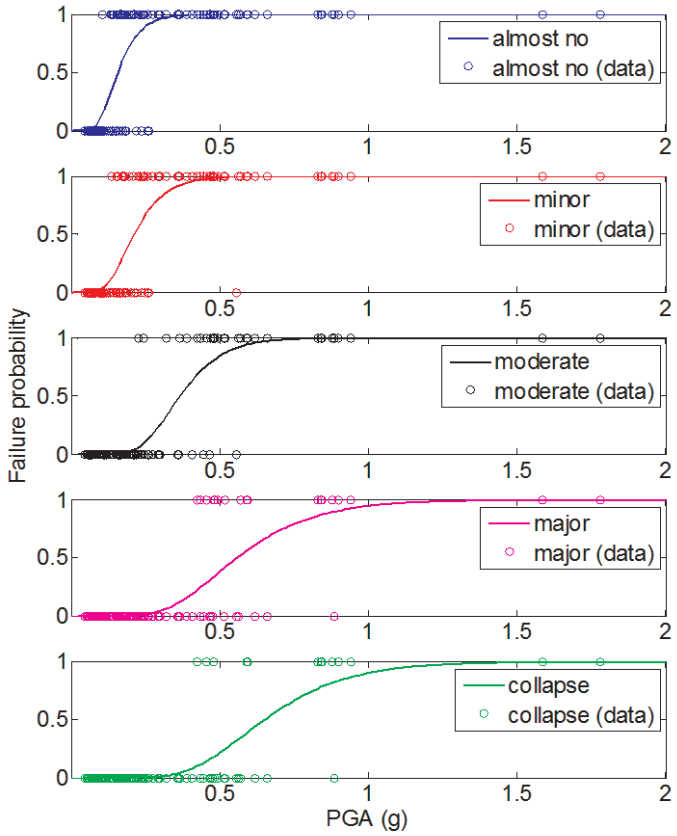

Figure 7.1. Fragility curve development of non-updated model (WN1).

At damage state 4, both observations and nonlinear time history analysis results have shown the very extreme level of structural damage. It is mentioned before that after yielding of columns, even buckling phenomena is observed in bent-3. Furthermore, nonlinear time history analysis results show that bent-3 reaches such ductility value of 18 which could be reasonably comprehended as structural failure. Therefore, Reliability estimations for damage state 4 is not conducted, as structure's residual life is no longer questionable.

In the Figure 7.2 fragility curves of non-updated model at initial state, state 1, is illustrated. It is convenient that failure probabilities of different fragility curves are hierarchically sequenced according to ductility levels. At a given PGA such as 0.2 g, "almost no" ductility demand level is expected with 75% probability whereas "minor"

and “moderate” ductility demand levels are only expected with probabilities of 45% and 3%, respectively. Expectance of “major” ductility is only 0.2%, and probability of ”collapse” at this stage is insignificant. Likewise, an earthquake of 0.4 g intensity would expect failure probabilities of 99%, 95%, 62%, 18%, and 8% according to ductility levels of almost no, minor, moderate, major, and collapse, respectively. Another focus on fragility estimates could be made at a PGA level of 0.6 g, where almost no, minor, moderate, major, and collapse curves would return probabilities of 99.98%, 99.7%, 95%, 58%, and 41%, respectively.

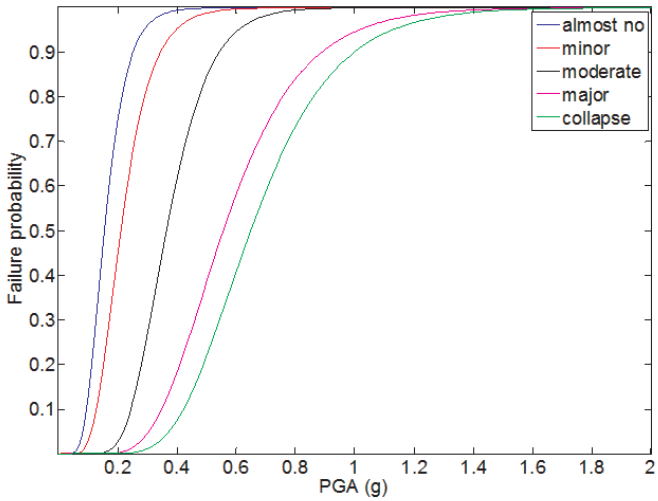

Figure 7.2. Fragility curves for non-updated model (WN1).

7.4. Effects of Model Updating and Structural Damage on Structural Reliability

Similarly, fragility curves for different damage states are obtained both for updated and non-updated models. Due to the fact that minor, moderate, and major fragility curves are adequately representative of non-updated and updated models at any damage state, only these curves are plotted in Figure 7.3 for comparison of non-updated and updated models at damage states 1, 2, and 3. It is shown that fragility curves of updated and non-updated models differ from each other for each damage state. Moreover, such difference becomes more distinguishable as damage severity increases. In addition, increasing failure probabilities, as a result of increasing damage

severity, could be tracked by the shift of any fragility curve to the left side of the graph with the increasing damage state. Table 7.1 and Table 7.2 contains more detailed information regarding failure probability findings from the Figure 7.3.

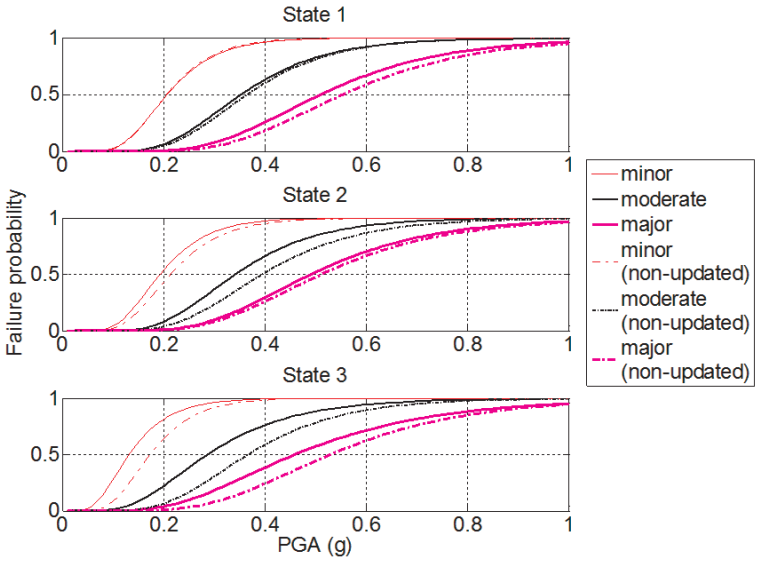

Figure 7.3. Fragility curves for updated and non-updated models.

In Table 7.2 the difference between structural reliability estimations of updated and non-updated models are investigated. Damage state 1 refers to the structural condition which has experienced no structural damage. According to reliability estimations of damage state 1, it is seen that system identification and finite element model updating results changes estimation results. It points out the fact that even without no damage initiation of structures, seismic performance evaluation of structures for a seismic event, which is based on nonlinear time history analysis only, may deviate from actual performance. Additionally, reliability estimations at damage state 2 and damage state 3, shows that such deviation could be much more prominent because that structural damage progression takes place. As a result, it is clearly observed that incorporation of structural system identification into structural reliability estimation process is significantly crucial for seismic performance assessment of structures.

In Table 7.3, the influence of structural damage on fragility curves is presented. It could be commented that damage progression results in a decrease in structural reliability values. This reveals that detection of present structural damage is essen-

Table 7.2. Effect of model updating on structural reliability in terms of failure probability.

	Damage State-1			Damage State-2			Damage State-3		
	FC: Minor PGA: 0.2 g	FC: Mod PGA: 0.4 g	FC: Major PGA: 0.6 g	FC: Minor PGA: 0.2 g	FC: Mod PGA: 0.4 g	FC: Major PGA: 0.6 g	FC: Minor PGA: 0.2 g	FC: Mod PGA: 0.4 g	FC: Major PGA: 0.6 g
Updated	0.464	0.635	0.669	0.537	0.663	0.703	0.813	0.759	0.714
Non-updated	0.469	0.605	0.589	0.431	0.515	0.665	0.641	0.588	0.624

tial for properly assessing structural performance. A scenario, that structural damage is not observable with conventional methods such as visual inspection and finite element analysis, emphasizes on the importance of system identification's contribution into performance assessment and evaluation. Otherwise, overestimation of structural reliability could cause misinterpretation of response predictions, and it may be the cause for catastrophic results.

Table 7.3. Effect of damage progression on structural reliability in terms of failure probability.

	Minor (0.2 g)			Moderate (0.4 g)			Major (0.6 g)		
	DS1	DS2	DS3	DS1	DS2	DS3	DS1	DS2	DS3
Updated	0.464	0.537	0.813	0.635	0.663	0.759	0.669	0.703	0.714

8. CONCLUSION

In this study, structural reliability estimation with the incorporation of structural system identification is carried out. A large scale, two-span, three-bent reinforced concrete bridge structure experienced large-scale shaking table tests which are characterized by sequentially increasing intensities. During the excitation tests, damage progression of a number of distinctive damage states, is documented with observations and measurements. Bent stiffness values and damping ratio are determined based on vibration-based identified structural parameters in time and frequency domain, and predicted based on nonlinear time history analysis. Eventually, based on identified (updated) and predicted (non-updated) parameters of each damage state, reliability estimations are accomplished by fragility curves. The conclusions are presented followings:

- Stiffness identification results show that there is a good correlation between frequency domain and time domain identification techniques used in this study, except few points such as the initial state, and Bent 2 at damage state 2. On the other hand, stiffness prediction results are different from identification results, especially in the initial phases of structural damage. For instance, according to state 2, in case time domain identification results are the reference, bent 1, bent 2, and bent 3 predictions due to nonlinear time history analysis are 51%, 30%, and 44%, respectively. In contrast, such values reduce significantly to 3%, 8%, and 6% for frequency domain identification. Nevertheless, identified and predicted parameters follow a similar trend, based on the qualitative definitions of damage progression.
- Damping ratio values, which are identified based on time domain identification and predicted based on damping-ductility relationship, significantly differ from each other. The increase in predicted damping ratio values is very steep, whereas identified damping ratios increase gradually with damage progression. At the initial state, damping values obtained from both methods are 5%. At the state 2, damping estimation of non-updated value starts to deviate from updated value

as only 13%. At the state 3 and 4, such deviation becomes 91% and 93%, respectively.

- In accordance with the differences in identified and predicted structural parameters, reliability estimation results of updated and non-updated models do not agree, as well. The most apparent observation is that non-updated reliabilities are almost always higher than updated reliabilities, for any damage state. Such statement refers to the danger of misleading reliability estimations without the presence of experimental information. This could lead to the overestimation of structural performance, which may result in wrong decisions regarding structures' faith. An instance to clarify this effect is that minor, moderate, and major failure probabilities of updated models are 97%, 66%, and 29%, whereas 95%, 55%, and 26% for non-updated models, for 0.4 g of state 2.
- Another conclusion drawn from fragility curves is that damage progression can be tracked based on residual reliabilities obtained from fragility curves. Failure probabilities moderate damage severity, at 0.4 g increases such as 63%, 66%, and 76%, with the progression of damage from state 1 to state 3. Similar behaviour can be observed for fragility curves of other damage severities.

In conclusion, it has been observed that reliability estimation based on vibration-based identified structural parameters are different than conventional pure analytical approaches. Therefore, sequentially applied system identification, finite element model updating, and reliability estimation procedures can result into the actual or at least accurate performance evaluation or damage assessment, and eventually, residual life of structures.

In order to improve the methodology, and the quality of work presented in this study, a number of recommendations are discussed regarding the future work:

- The reliability estimations made in this study are based on a set of earthquake records which belong to 1994 Northridge Earthquake. Therefore, another set of records could lead different results. For this purpose, different sets of records could be used to observe the differences. Such differences could be related with

strong ground motion parameters which enables to achieve a generalized solution.

- Computation cost of time-history analysis is very high, which is a burden for a parametric study. It obliges to reduce the parameter range and discretization number of parameters, to conduct an analysis within a reasonable amount of time. Development of smarter algorithms for system identification would reduce the computational time and make it possible to obtain results closer to the exact values.
- Nonlinearity in structures is an aspect of engineering which is still ambiguous to a great extent. Therefore, different approaches of nonlinearity could be tested whether they result in similar results. In fact, more advanced analytical approaches exist in the literature which may represent structural response better.
- A further suggestion is that nonlinearity in identification techniques are highly emphasized by pioneer structural health monitoring researches. Following studies examining this phenomena contribute greatly to the literature.

REFERENCES

ACI Commitee 318, 2008, "Building Code Requirements for Structural Concrete (ACI 318-08) and Commentary", *American Concrete Institute*, Farmington Hills, MI.

Ang, A.H-S. and W.H., Tang, 1975, "Probability Concepts in Engineering Planning and Design Volume I - Basic Principles", Wiley, New York.

Ang, A.H-S. and W.H., Tang, 1984, "Probability Concepts in Engineering Planning and Design Volume II - Decision, Risk, and Reliability", *Wiley*, New York.

Banerjee, S. and M., Shinozuka, 2008, "Experimental Verification of Bridge Seismic Damage States Quantified by Calibrating Analytical Models with Empirical Field Data", *Earthquake Engineering and Engineering Vibration*, Vol. 7, No. 4, pp. 383-393.

Banerjee, S. and M., Shinozuka, 2008, "Integration of Empirical, Analytical and Experimental Seismic Damage data in the Quantification of Bridge Seismic Damage States", *Proceedings, Concrete Bridge Conference HPC - Safe, Affordable, and Efficient*, May 4-7, St. Louis, Missouri.

Beck, J.L. and L.S., Katafygiotis, 1998, "Updating Models and Their Uncertainties. I: Bayesian Statistical Framework", *Journal of Engineering Mechanics*, Vol. 124, No. 4, pp. 455-461.

Brincker, R., L., Zhang and P., Andersen, 2001, "Modal Identification of Output-Only Systems Using Frequency Domain Decomposition", *Smart Materials and Structures*, No. 12, pp. 441-445.

Brownjohn, J.M.W., 2007, "Structural Health Monitoring of Civil Infrastructure", *Philosophical Transactions of the Royal Society*, Vol. 3, No. 65, pp. 589-622.

BS EN 1992-1-1 2005, "Eurocode 2: Design of Concrete Structures", *British Standard Institution*, London.

Carden, E.P., and P., Fanning, 2004, "Vibration-Based Condition Monitoring-A Review", *Structural Health Monitoring*, Vol. 3, No. 4, pp. 355-377.

Catbas, F.N., M., Susoy and D.M., Frangapol, 2008, "Structural Health Monitoring and Reliability Estimation: Long Span Truss Bridge Application with Environmental Monitoring Data", *Engineering Structures*, No. 30, pp. 2347-2359.

Celebi, M. and E., Safak, 1991, "Seismic Response of Transamerica Building. I: Data and Preliminary Analysis", *Journal of Structural Engineering*, Vol. 117, No. 8, pp. 2389-2404.

Chopra, A., 2007, "Dynamics of Structures Theory and Applications to Earthquake Engineering", *Prentice Hall International Series in Civil Engineering and Engineering Mechanics.*, Upper Saddle River, NJ 07458.

Doebling, S.W., C.R., Farrar, M.B., Prime and D.W., Shevitz 1996, "Damage Identification and Health Monitoring of Structural and Mechanical Systems from Changes in Their Vibration Characteristics: A Literature Review", *Los Alamos National Laboratory Report*, LA-13070-MS.

Ewins, D.J., 2000, "Modal Testing: Theory, Practice and Application", *Research Studies Press, Ltd.*, Baldock, Hertfordshire, England.

Feng, M.Q., D.K., Kim, J.H., Yi and Y.B., Chen, 2003, "Baseline Models for Bridge Performance Monitoring", *Journal of Engineering Mechanics*, vol. 131, No. 5, pp. 562-569.

Frangopol, D.M., A., Strauss and S., Kim, 2008, "Bridge Reliability Assessment Based on Monitoring", *Journal of Bridge Engineering*, Vol. 13, No. 3, pp. 258-270.

Friswell, M.I., J.E., Mottershead and H., Ahmadian, 2001, "Finite Element Model

Updating Using Experimental Test Data: Parametrization and Regularization", *Philosophical Transactions of the Royal Society*, A 359, 169-186.

Gardoni, P., A.D., Kiureghian and K.M., Mosalam, 2002, "Probabilistic Models and Fragility Estimates for Bridge Components and Systems", *Pasific Earthquake Engineering Research Center*, University of California, Berkeley.

Ghanem, R., and M., Shinozuka 1995, "Structural-System Identification. I: Theory", *Journal of Engineering Mechanics*, Vol. 121, No. 2, pp. 255-264.

Johnson, N.S., M., Saiidi and D.H., Sanders, 2006, "Large-Scale Experimental and Analytical Seismic Studies of a Two-Span Reinforced Concrete Bridge System", Report No. CCEER-06-02, *Center for Earthquake Engineering Research*, University of Nevada, Reno, NV.

Katafygiotis, L.S. and J.L., Beck 1998, "Updating Models and Their Uncertainties. II: Model Identifiability", *Journal of Engineering Mechanics*, Vol. 124, No. 4, pp. 463-467.

Kowalsky, M.J., 2002, "A Displacement-Based Approach for the Seismic Design of Continuous Concrete Bridges", E*Arthquake Engineering and Structural Dynamics* No. 31 pp. 719-747.

Kozin, F. and H.G., Natke, 1986, "System Identification Techniques", *Structural Safety*, Vol. 3 No. 3-4, pp. 269-316.

Ljung, L., 1999, "System Identification Theory for the User", *Prentice Hall Information and System Sciences Series*, Upper Saddle River, NJ 07458.

Lus, H., R., Betti and R.W., Longman, 1999, "Identification of Linear Structural Systems Using Earthquake-Induced Vibration Data", *Earthquake Engineering and Structural Dynamics*, No. 28, pp. 1449-1467.

Maia, N.M.M. and J.M.M., Silva, 2001, "Modal Analysis Identification Techniques",

Philosophical Transactions of the Royal Society, A 359, 29-40.

Masri, S.F., A.W., Smyth,A.G., Chassiakos, T.K., Caughey and N.F., Hunter, 2000, "Application of Neural Networks for Detection of Changes in Nonlinear Systems", *Journal of Engineering Mechanics*, Vol. 126, No. 7, pp. 666-676.

Matlab, 2009, "The Language of Technical Computing", *The MathWorks*, Inc.

Mazzoni, S., F., McKenna, M.H., Scott and G.L., Fenves, 2007, "OpenSees Command Language Manual", *University of California*, Berkeley, CA.

McKenna, F., G.L., Fenves and M.H., Scott, 2004, "OpenSees: Open System for Earthquake Engineering Simulation.Pacific Earthquake Engineering Research Center" *University of California*, Berkeley, CA.

Melchers, R.E., 1999, "Structural Reliability Analysis and Prediction", *Wiley*, New York.

Moaveni, B., X., He, J.P., Conte and J.I., Restrepo, 2010 "Damage Identification Study of a Seven-Story Full-Scale Building Slice Tested on the UCSD-NEES Shake Table", *Structural Safety* Vol. 32, No. 5, pp. 347-356.

Park, Y-J., A.H-S, Ang and Y.K., Wen, 1985, "Seismic Damage Analysis of Reinforced Concrete Buildings", *Journal of Structural Engineering ASCE*, Vol. 111, No. 4, pp. 740-757.

PEER Strong Motion Database, 2005, "The Pasific Earthquake Engineering Research" Center and the University of California.

Priestley, M.J.N., F., Seible and G.M., Calvi, 1996, "Seismic Design and Retrofit of Bridges", *Wiley*, New York.

Safak, E. and M., Celebi, 1991, "Seismic Response of Transamerica Building. 2: System Identification", *Journal of Structural Engineering*, Vol. 117, No. 8, pp. 2405-2425.

Safak, E., 1989, "Adaptive Modeling, Identification, and Control of Dynamic Structural Systems. I: Theory", *Journal of Engineering Mechanics*, Vol. 115, No. 11, pp. 2386-2405.

Safak, E., 1989, "Adaptive Modeling, Identification, and Control of Dynamic Structural Systems. 2: Applications", *Journal of Engineering Mechanics* vol. 115, No. 11, pp. 2406-2426.

Safak, E., 1991, "Identification of Linear Structures Using Discrete-Time Filters", *Journal of Structural Engineering* Vol. 17, No. 10, pp. 3064-85.

SAP 2000, "Static and Dynamic Analysis of Structures Advanced 10.0.1". Computers and Structures, Inc. 1995 University Ave. Berkeley, CA 94704.

Shinozuka, M. and R., Ghanem, 1995, "Structural-System Identification. 2: Experimental Verification", *Journal of Engineering Mechanics*, Vol. 121, No. 2, pp. 265-273.

Shinozuka, M., M.Q., Feng and H-K., Kim, 2000, "Nonlinear Static Procedure for Fragility Curve Development", *Journal of Engineering Mechanics* vol. 126, No. 12, pp. 1287-1295.

Shinozuka, M., M.Q., Feng, J. Lee and T., Naganuma, 2000, "Statistical Analysis of Fragility Curves", *Journal of Engineering Mechanics*, Vol. 126, No. 12 pp. 1224-1231.

Shinozuka, M., C-B., Yun and H., Imai, 1982, "Identification of Linear Structural Dynamic Systems",*Journal of Engineering Mechanics*, Vol. 108, No. 6 pp. 1371-1390.

Singhal, A. and A.S., Kiremidjian, 1998, "Bayesian Updating of Fragilities with Application to RC Frames", *Journal of Structural Engineering ASCE*, Vol. 124, No. 8, pp. 922-929.

Skolnik, D., L., Ying, Y.,Eunjong and J.W., Wallace, 2006, "Identification, Model Updating, and Response Prediction of an Instrumented 15-Story Steel-Frame Building", *Earthquake Spectra* Vol. 22, No. 3, pp. 781-802.

Sohn, H., C.R., Farrar, F.M., Hemez, D.D., Shunk, D.W., Stinemates, B.R., Nadler and J.J., Czarnecki, 2004, "A Review of Structural Health Monitoring Literature", *Los Alamos National Laboratory Report*, LA-13976-MS.

Turkish Standards Institute, "TS-500 Building Code Requirements for Structural Concrete", Ankara.

Yazgan, U. and A., Dazio, 2011, "Simulating Maximum and Residual Displacements of RC Structures: I. Accuracy", *Earthquake Spectra*, Vol. 27, No. 4, pp. 1187-1202.

Yazgan, U., and A., Dazio, 2011, "Simulating Maximum and Residual Displacements of RC Structures: II. Sensitivity", *Earthquake Spectra*,Vol. 27, No.4, pp.1203-1218.

Yun, C-B. and M., Shinozuka, 1980, "Identification of Nonlinear Structural Dynamic Systems", *Journal of Structural Mechanics*, Vol. 8, No. 2, pp. 187-203.